FABRICATION AND CHARACTERIZATION OF ELECTROSPUN POLY-CAPROLACTONE-GELATIN COMPOSITE CUFFS FOR TISSUE ENGINEERED BLOOD VESSELS

A Thesis

Submitted to the faculty of the

WORCESTER POLYTECHNIC INSTITUTE

In partial fulfillment of the requirements for the

Degree of Master of Science
In Biomedical Engineering

April 2, 2015

By

Elizabeth L Mayor

Anjana Jain, Ph.D.
Assistant Professor
Department of Biomedical Engineering
Worcester Polytechnic Institute
Committee Member

George D. Pins, Ph.D.
Associate Professor
Department of Biomedical Engineering
Worcester Polytechnic Institute
Committee Member

Marsha W. Rolle, Ph.D.
Associate Professor
Department of Biomedical Engineering
Worcester Polytechnic Institute
Thesis Advisor

Contents

Table of Figures v

Table of Tables vi

Acknowledgements vii

Abstract viii

Chapter 1. Introduction and objectives 9

1.1 Objective one: Fabricate and characterize cuff material 11

1.2 Objective two: Measure SMC response to cuff materials 11

1.3 Objective three: Evaluate cuff integration with 3D cell derived tissue tubes 12

Chapter 2. Background and literature review 13

2.1 Tissue engineered vascular graft background and need 13

2.1.1 Clinical need for tissue engineered vascular grafts 13

2.1.2 Advantages and needs in ring fused tube system 13

2.2 Cuffs in vascular engineering 14

2.2.1 Sewing cuffs: uses and applications 14

2.2.2 Cuffs as manipulation tools for tissue engineered blood vessels 15

2.3 Electrospinning fabrication method 16

2.3.1 Electrospinning theory and advantages 16

2.3.2 Electrospinning for vascular grafts 19

2.4 Cuff material choice 20

2.4.1 Natural and synthetic blends 20

2.4.2 Coating and co-spinning 21

2.5 Cuff evaluation methods 23

2.5.1 Electrospun morphology: Porosity, pore size and fiber diameter 23

2.5.2 Mechanical properties 24

2.5.3 Attachment of SMC to cuff materials 25

2.5.4 Outgrowth of SMC over cuff materials 25
2.5.5 Cuff tissue integration 25
Chapter 3. Fabricate and characterize cuff scaffold materials 27
3.1 Introduction 27
3.2 Methods 27
3.2.1 Fabrication methods 27
3.2.2 Characterization methods 31
3.3 Results 33
3.3.1 Electrospinning optimization 33
3.3.2 Fiber diameter 36
3.3.3 Pore size and porosity 37
3.3.4 Gelatin visualization 38
3.3.5 Mechanical testing 39
3.4 Discussion 40
3.4.1 Fabrication optimization 40
3.4.2 Scaffold morphology 41
3.4.3 Mechanical properties 43
3.4.4 Impact of material properties on cuff integration 44
Chapter 4. Cellular attachment and outgrowth on cuff materials 46
4.1 Introduction 46
4.2 Methods 46
4.2.1 RASMC culture 46
4.2.2 Cellular attachment assay 46
4.2.3 Outgrowth assay 48
4.3 Results 49
4.3.1 Attachment of RASMC to cuff materials 49

4.3.2 Outgrowth 50
4.4 Discussion 52
Chapter 5. Cuff integration with 3D cell derived tissues 55
5.1 Introduction 55
5.2 Methods 55
5.2.1 Ring formation 55
5.2.2 Tube fusion 56
5.2.3 Longitudinal pull to failure 56
5.2.4 Histology 57
5.3 Results 58
5.3.1 Longitudinal pull to failure 58
5.3.2 Histology 59
5.4 Discussion 61
5.4.1 Mechanical testing 61
5.4.2 Histological evaluation 61
Chapter 6. Conclusions and future work 62
6.1 Conclusions 62
6.1.1 Cuffs as tools for developing tissue engineered blood vessels 62
6.1.2 Cospinning is an effective method for gelatin incorporation within electrospun PCL materials 62
6.1.3 Predicting material integration with 3D cell derived tissues 64
6.2 Future work 64
6.2.1 Further analyze differences in material properties between experimental cuff materials 64
6.2.2 Analyze the impact of variability in electrospun materials 65
6.2.3 Improve resolution of testing protocols 66

6.2.4 Broader applications of electrospun cuffs 67

Citations.....68

Appendix A: Attachment assay standard curves 75

Appendix B: CAD drawings of custom mechanical testing grips 76

Table of Figures

Figure 1: Overview of the application of cuffs in TEBV fabrication 2
Figure 2: Electrospinning schematic. 18
Figure 3: Gelatin Incorporation methods for fabricating blended cuffs 23
Figure 4: Electrospinning setup. 28
Figure 5: Gelatin coating process 30
Figure 6: DiameterJ fiber diameter measurements 31
Figure 7: Fiber diameter parameter screening 35
Figure 8: Gelatin coating optimization 36
Figure 9: Fiber diameter of PCL and PCL gelatin composites 37
Figure 10: Porosity. 38
Figure 11: Gelatin visualization 38
Figure 12: Representative stress strain curves 39
Figure 13: Mechanical properties 40
Figure 14: Attachment assay sample preparation 47
Figure 15: Ibidi chamber seeding 48
Figure 16: Attachment of RASMC to electrospun materials 49
Figure 17: Outgrowth representative images 51
Figure 18: RASMC outgrowth over 36 hours 52
Figure 19: Maximum RASMC outgrowth 52
Figure 20: Custom grip loading 56
Figure 21: Sample modes of failure 57
Figure 22: RASMC ring/cuff tubes post longitudinal pull to failure 58
Figure 23: Maximum longitudinal load 59

Table of Tables

Table 1: Cuff material design targets 11
Table 2: Parameter ranges for electrospinning optimization 29
Table 3: Taylor cone optimization 34
Table 4: Theoretical pore size 38
Table 5: Resources, cost and time required for fabricating gelatin incorporated cuffs 63

Acknowledgements

I would like to thank Prof. Marsha Rolle for being a wonderful advisor to me; her advice and guidance throughout this project have been invaluable.

I would also like to thank my committee members, Prof. Anjana Jain and Prof. George Pins, for their feedback and insights on this project. I would especially like to thank Prof. Jain for collaborating with us on electrospinning of the materials by providing the materials, equipment, and advice needed to get this project going.

I would also like to thank all the graduate and undergraduate members of the Rolle lab for all their help over the last few years. I would like to especially thank Zoe Reidinger and Hannah Strobel for all of their help and encouragement.

I am grateful to Alex Beliveau for teaching me electrospinning and how to work with electrospun fibers and for answering my endless questions about the process. Thank you to Katrina Hansen and Emily Abbate for ethylene oxide sterilizing all of my materials. Thank you to Jon Grasman and Prof. Boquan Li in the mechanical engineering department for all their help with SEM imaging. Thank you to Dr. Nathan Hotaling at the NIST for giving me early access to their DiameterJ software. Thank you to Matt DiPinto in Washburn shops for helping with the fabrication of the custom motor couple.

Lastly, I would thank my family and friends for all their love and support, and for the many words of encouragement over the years.

Abstract

Strong, durable terminal regions that can be easily handled by researchers and surgeons are a key factor in the successful fabrication of tissue engineered blood vessels (TEBV). The goal of this study was to fabricate and characterize electrospun cuffs made of poly-caprolactone (PCL) combined with gelatin that reinforce and strengthen each end of cell-derived vascular tissue tubes. PCL is ideal for vascular tissue engineering applications due to its mechanical properties; however, PCL alone does not support cell attachment. Therefore, we introduced gelatin, a natural matrix-derived protein, into the electrospun material to promote cell adhesion. This work compared the effects of two different methods for introducing gelatin into the PCL materials: gelatin coating and gelatin co-electrospinning. Porosity, pore size, fiber diameter, and mechanical properties of the electrospun materials were measured in order to compare the features of gelatin PCL composites that have the greatest impact on cellular infiltration. Porosity was quantified by liquid intrusion, fiber diameter and pore size were measured using scanning electron microscopy, and tensile mechanical testing was used to evaluate strength, elastic modulus, and extensibility. Attachment and outgrowth of smooth muscle cells onto cuff materials was measured to evaluate differences in cellular interactions between materials by using a metabolic attachment assay and a cellular outgrowth assay. Finally, cuffs were fused with totally cell-derived TEBV and the integration of cuffs with tissue was evaluated by longitudinal pull to failure testing and histological analysis. Overall, these cuffs were shown to be able to add length and increase strength to the ends of TEBV for tube cannulation and manipulation during *in vitro* culture. In particular, PCL:gelatin cospun cuffs were shown to improve cellular attachment and cuff fusion compared to pure PCL cuffs, while still increasing the strength of the TEBV terminal ends.

Chapter 1. Introduction and objectives

The focus of this work is to fabricate cuffs for tissue engineered vascular grafts to facilitate handling and cannulation for bioreactor culture and mechanical testing. Our lab creates engineered vascular tissue through self-aggregation of vascular smooth muscle cells (SMC) into toroidal rings. These rings can then be fused to form tubes that can be used as tissue engineered blood vessels (TEBV), but these tubes can be too fragile to easily manipulate during the early stages of production and *in vitro* culture. Incorporating synthetic cuffs onto the ends of these tubes may improve the ease of manipulation of tubular tissue constructs during culture and testing by extending the length, and adding strength at the ends of the constructs.

In the work described in this thesis, cuffs were made of a synthetic polymer material electrospun into a tubular shape of the same diameter as the tissue (2mm inner diameter). Short, 2-5mm segments were attached to the ends of cell-derived tubular constructs and integrated through cellular infiltration from adjacent cell-derived ring segments. Cuffs provide a region for handling the constructs during the tissue production process. Cuffs provide a strong, but ultimately sacrificial end segment of a tissue tube that can increase ease of cannulation for securing of the graft onto bioreactors or testing devices without the need for long segments of engineered tissue. These cuff materials can be removed prior to implantation. Figure 1 shows an overview of the process of using cuffs, and a schematic of how cuffs and tissue are fused.

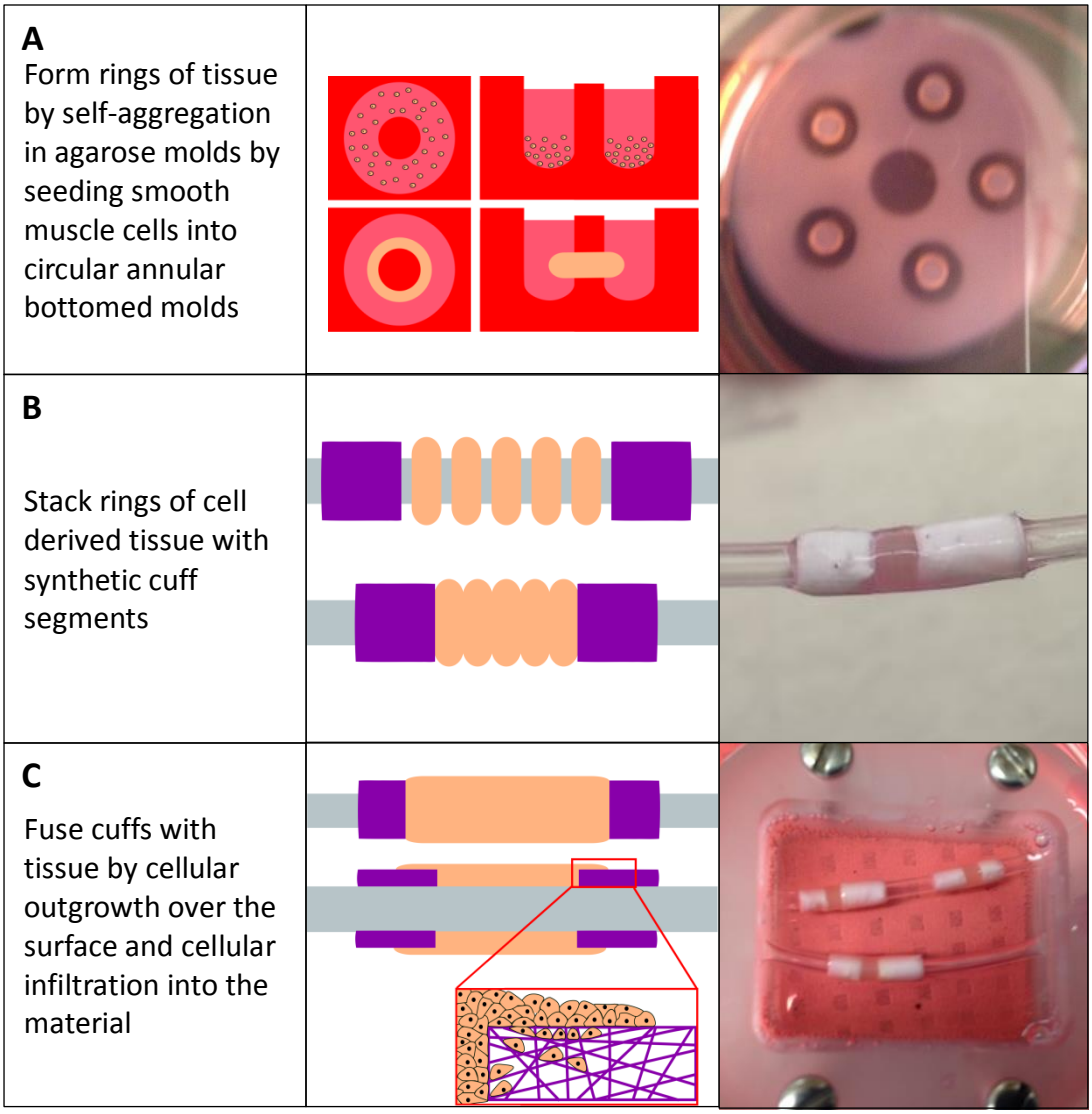

Figure 1: Overview of the application of cuffs in TEBV fabrication. Cartoons and images illustrate how cuffs were incorporated with self-assembled cell rings to form TEBV. **A)** Form completely cell derived tissue rings through self-aggregation in agarose molds, top view and side view shown in cartoon, top view of 5 rat aortic smooth muscle cell rings shown in image. **B)** Two electrospun synthetic PCL cuffs and 5 smooth muscle cell rings stacked on silicone tubing, shown in cartoon and image. **C)** Tubes fused with PCL cuffs after 7 days in culture shown in cartoon and image, cross section shown in cartoon with inset showing cellular outgrowth and infiltration

In order to create these cuffs for TEBV, we have identified the following objectives:

1. Fabricate and characterize the cuff material
2. Measure SMC response to cuff materials
3. Evaluate cuff integration with 3D cell derived tissue tubes

1.1 Objective one: Fabricate and characterize cuff material

The goal of this objective was to select an appropriate material and method to fabricate cuffs, and characterize the material properties and structure of the cuff material. Electrospinning was chosen to fabricate cuffs as it is a versatile method for the fabrication of nanofibrous scaffolds that is compatible with a wide variety of materials. Electrospun scaffolds can be made of natural materials, which support excellent cellular integration, and synthetic materials, which often have mechanical properties tailored to the tissue engineering application. We hypothesized that by blending natural and synthetic materials it would be possible to maintain the strength of a purely synthetic scaffold while improving cellular attachment and infiltration using a natural material. Here, we have compared two methods for blending natural proteins into synthetic electrospun cuffs: protein coating and protein co-electrospinning. Then we compared the effects of these two incorporation methods on features critical to (1) vascular cell attachment and infiltration: pore size, porosity, and fiber diameter, and (2) mechanical properties important to functionality as a cuff: material stiffness (elastic modulus) and material strength (ultimate tensile strength).Table 1 lists target values for these parameters based on scaffolds designed for tissue engineered blood vessels.

Table 1: Cuff material design targets.

Material feature	Evaluating method	Design specification
Pore size	SEM imaging and theoretical fiber diameter based modeling	10μm or larger[1]
Porosity	Liquid intrusion	>70% Void fraction[2]
Fiber diameter	SEM imaging	Average greater than 200μm[3]
Ultimate tensile strength	Instron tensile testing	Greater than cell derived ring constructs
Elastic modulus	Instron tensile testing	Closely matched to cell-derived ring constructs

1.2 Objective two: Measure SMC response to cuff materials

After establishing fabrication methods and material properties of cuffs in objective one, the aim of objective two was to compare SMC responses on the synthetic and protein blended materials, particularly outgrowth and attachment. We hypothesized that these two features of

the SMC response can be used as predictors of successful cuff tissue integration. Therefore, quantitative assays were used to screen potential cuff materials based on cellular attachment and outgrowth of smooth muscle cells by direct seeding methods, and determine which material supports the greatest SMC attachment and outgrowth. These assays were designed to compare the behavior of SMC seeded directly onto flat sheets of these materials, in order to use that data to predict three dimensional interactions between SMC in totally cell derived rings and cuff materials. We hypothesized that materials with incorporated proteins would support much higher cellular outgrowth and infiltration than pure synthetic materials, and that these findings would correlate with 3D cuff integration studies performed for objective 3.

1.3 Objective three: Evaluate cuff integration with 3D cell derived tissue tubes

Following direct seeding assays, the natural and synthetic blended materials were tested in the 3D cell derived ring system. Cuff materials were fused with SMC rings and the extent of integration between the cuffs and tissue was compared between materials. In order to evaluate integration, the outgrowth and infiltration of SMC into cuffs from tissue engineered vessels was measured through histological analysis. The strength of the bond between SMC tissue and cuffs was evaluated using longitudinal pull to failure testing. This allowed not only for a comparison of the three materials, but also to determine which previously measured material properties were the best predictor of successful cuff integration. Results from the evaluation of structure and material properties completed in objective one, and the SMC response evaluated in objective two was then compared to 3D results to determine the correlation between specific material properties and cuff integration. These integration experiments were also able to establish if protein incorporation is an effective method for improving cuff performance, and if there are differences in cuff performance based on the protein incorporation method: coating or cospinning.

Chapter 2. Background and literature review

2.1 Tissue engineered vascular graft background and need

2.1.1 Clinical need for tissue engineered vascular grafts

Cardiovascular disease is the leading cause of death worldwide, and a large portion of those deaths are directly related to vascular diseases[4,5]. A large majority of these patients require surgical intervention to replace diseased or damage vasculature[6]. For example, nearly 400,000 bypass grafts are performed each year in the U.S.[5]. For these procedures, the gold-standard graft materials, autografts (usually internal mammary artery, saphenous vein, and radial artery) are not always available. In fact, no suitable autograft can be found in nearly one third of patients[6]. An alternative is needed, opening the door for vascular tissue engineering to develop suitable options for these patients.

Many groups are working towards developing a tissue engineered blood vessel, using combinations of unique biomaterials, cells and cell derived products[6]. Our lab has developed a novel modular ring system that has great potential for fabricating totally cell derived vascular constructs[7]. This method depends on the fabrication of self-assembled cell rings which can be stacked and fused in culture to form tubes. Briefly, smooth muscle cells are seeded as a high density cell suspension into ring-shaped agarose wells with central posts. After 24 hours, these cells aggregate and contract around the central post to form rings. After a period of culture as rings, they can be removed from the agarose wells and stacked on silicone tubing for continued culture as a tube construct, during which time individual rings fuse together and form entirely cell-derived tissue tubes.

2.1.2 Advantages and needs in ring fused tube system

Using the ring fusion system provides unique advantages over other systems. One of the greatest advantages is that the tissue formed is entirely composed of cells and cell-derived matrix, without the need for external scaffold material. The system is highly versatile due to the modular method of fabrication; each individual ring can be viewed as a single modular unit in the tube fusion system, allowing for the incorporation of rings with different properties in the

same tube. Rings of different cell types or treatment groups can be combined to form tubes with spatially defined regions of different properties. These tubes are also of versatile dimensions; length can easily be modified by incorporating more or less rings, and internal diameter can easily be changed by using an agarose mold of differing dimensions[7].

However, with the unique advantages of this system come unique challenges. As tissues are completely cell-derived, during the early stages of tube culture they can be difficult to manipulate directly without damaging the tissue when transferring tubes between bioreactors and testing devices. We have also found that many of the standard procedures for testing tissue tubes, in particular burst-pressure testing and longitudinal tensile testing, require sacrificial terminal regions of the tubes. This means that a great deal of labor, cells and reagents must be used to fabricate tissue material that is ultimately sacrificial during testing and culture.

Based on the current needs of the system, it is has been shown that the ends of fused ring-tubes must be reinforced and lengthened to facilitate manipulation and testing of the constructs. Here we explored a method for accomplishing this by taking advantage of the unique modular capabilities of the ring fused tube system. By incorporating synthetic ring units at the ends of the cell-derived tubes, we created strong sacrificial regions of synthetic material that can be used by researchers to manipulate the tubes without damaging the tissue while mounting samples in testing devices and bioreactors. These synthetic rings or "cuffs" were fused directly to the cell rings via cellular integration in the tube fusion system. For cuffs to be successfully used in our TEBV system, the cuffs should be stronger than the cell-derived portion of the tissue to add strength to terminal regions, and be able to fuse robustly with cell derived tissue to integrate seamlessly with cell derived rings.

2.2 Cuffs in vascular engineering

2.2.1 Sewing cuffs: uses and applications

In the surgical setting, sewing cuffs have been used in cardiovascular implants, namely for prosthetic mitral valves and prosthetic aortic valves, to accomplish similar design goals to those proposed for our TEBV cuffs[8]. These cuffs provide a point for anchoring sutures to the prosthesis without damaging the material of the valve. It also provides structural integrity at

the implant site, by using a stiffening ring to maintain the prosthesis in the appropriate circular shape during implantation. In order for these sewing cuffs to be effective, they must also prevent damage to the prosthesis during handling, assembly and implantation [9]. "Sewing cuffs" have been used in vascular grafts, and while these are still anastomotic connectors placed at the ends of grafts, the purpose for their use and materials used are different than sewing cuffs used for prosthetic valves. Vascular sewing cuffs are segments of vessel used to minimize compliance mismatch between the graft and native vessel. For synthetic grafts, the compliance mismatch can be significant, leading to decreased graft patency[10]. In these cases, a short segment of venous tissue, a Miller cuff, is placed interpositionally between graft and native artery, is used to mitigate the compliance mismatch and minimize the risk of hyperplasia[11]. Synthetic sewing cuffs have been shown to be useful for the purpose of minimizing the difficulty of the surgical techniques needed for graft implantation by providing support at the anastomoses, but their use is not widely accepted [12]. Therefore, in a surgical setting, the features important for fabricating a successful cuff are to provide a strong location for manipulation and suturing while matching the compliance of native tissue.

2.2.2 Cuffs as manipulation tools for tissue engineered blood vessels

Recently, the use of sewing cuffs has been applied to tissue engineered vascular grafts in order to take advantage of the benefits sewing cuffs have provided for both heart valve implantation and vascular graft implantation. For example, Watanabe et al, formed vascular grafts known as "biotubes " through tissue encapsulation of a silicone mandrel, but found that their tissue engineered vascular grafts were impossible to implant using traditional microsurgery techniques[13]. They hypothesized that synthetic vascular cuffs were needed to reinforce the ends of the grafts to provide a more structurally sound region that maintains the correct circular dimensions of the anastomoses. The sewing cuffs were formed using polyurethane sponge tubing and attached to biotubes by cellular infiltration and encapsulation. These cuffs provided a region to grip and manipulate the biotubes during implantation[14,15]. However, the cuff segments were permanent, as the polyurethane was not biodegradable.

The need for cuffs has been recognized in other tissue engineered vascular systems as well; even vessels designed with internal synthetic scaffolding require cuffs for reinforcement

of the terminal regions. The Niklason group developed a tissue engineered blood vessel system where Smooth muscle cells are seeded into a PGA mesh scaffold that must then be sutured in place in a pulsatile flow bioreactor for mechanical stimulation[16]. In order to facilitate placement of vessels into the bioreactor, Huang et al used Dacron cuffs sutured to the PGA mesh that served as the scaffold for tissue engineered vessels[17]. These cuffs provided a location to suture the vessels onto the cannulas of the bioreactor [17]. However, as with the polyurethane cuffs used in the biotube system, these cuffs were not biodegradable. These cuffs were attached to TEBV constructs via suture material, not through cellular integration. Syedain et al discuss the use of PLA sewing cuffs in their tissue engineered blood vessel system[18]. Briefly, vessels are fabricated by encapsulating fibroblasts in fibrin gels seeded into a tubular mold. As with the previously described systems, in order to manipulate and suture TEBV, sewing cuffs were incorporated into the vessels. Therefore, PLA cuffs were placed into seeding molds and fused with fibrin/fibroblast vessels. These cuffs improved the suture retention strength of their grafts such that they were comparable with internal mammary artery[18]. However, they plan to eliminate the cuffs from their long term production strategy to eliminate synthetic materials from their system[18].

Overall, cuffs have been shown to be effective at reinforcing the ends of TEBV constructs, minimizing compliance mismatch, and facilitating surgical implantation or the manipulation of constructs in bioreactors and testing devices. By applying the knowledge of the previous use of cuffs, we developed cuff materials that will perform best for cell-derived ring TEBV system *in vitro*.

2.3 Electrospinning fabrication method

2.3.1 Electrospinning theory and advantages

Since the potential benefits of using cuffs have been established, a fabrication method for the cuffs must be chosen for the self-assembled ring-fusion system. Previous methods for fabricating cuffs for tissue engineered vessels have included woven fabrics, sponges, and commercially available materials[13,17,18]. However, in the previous instances of using cuffs in TEBV, cuff and tissue fusion was accomplished very differently than the cellular outgrowth and

infiltration method proposed here. For PLA cuffs used by the Tranquillo lab, the material was embedded directly into the fibrin gel and was chosen for the increased suture retention strength over the fibrin alone, rather than for cellular attachment properties[18]. Similarly, PU cuffs were embedded into "biotube" vessels by tissue encapsulation. Cuffs cannot be embedded in this way for TEBV formed by fusing rings, however, as there is no mold or material for cuffs to be embedded in, in our system. The cuffs used by the Niklason group were attached to a PGA mesh TEBV using suture material, however as with embedding, cuffs would not be well fused with cell derived rings using this method. Therefore, we chose to design and fabricate cuffs with tissue-cuff fusion in mind. Cuff materials must support significant cellular attachment, outgrowth, and infiltration in order to fuse well with cell-derived rings. With these criteria, we elected to explore electrospinning to create a highly porous scaffold, to allow for cellular infiltration, with a high surface area that provides many cellular attachment points.

Electrospinning is a simple, inexpensive, well-established and versatile method for fabricating scaffold materials. Electrospinning is a process for fabricating non-woven nano and microfiber meshes that has been used since 1934[19]. However, it is only in the last 15 years that this method has been become more widely used for biomedical applications[20]. The premise of electrospinning is based on using a jet of polymer dissolved in organic solvent drawn through the air using a strong electric field between a charged source (syringe in a syringe pump) and a grounded collector, creating a whipping jet of nanofibers as the solvent is evaporated into the air, as shown schematically in Figure 2[21]. This process can be adapted to a wide array of polymers and solvents, and many parameters of the fibers can be controlled, including fiber size, morphology and density, as well as geometry, based on adaptations of collector shape, electric field strength, flow rate and collector distance[22].

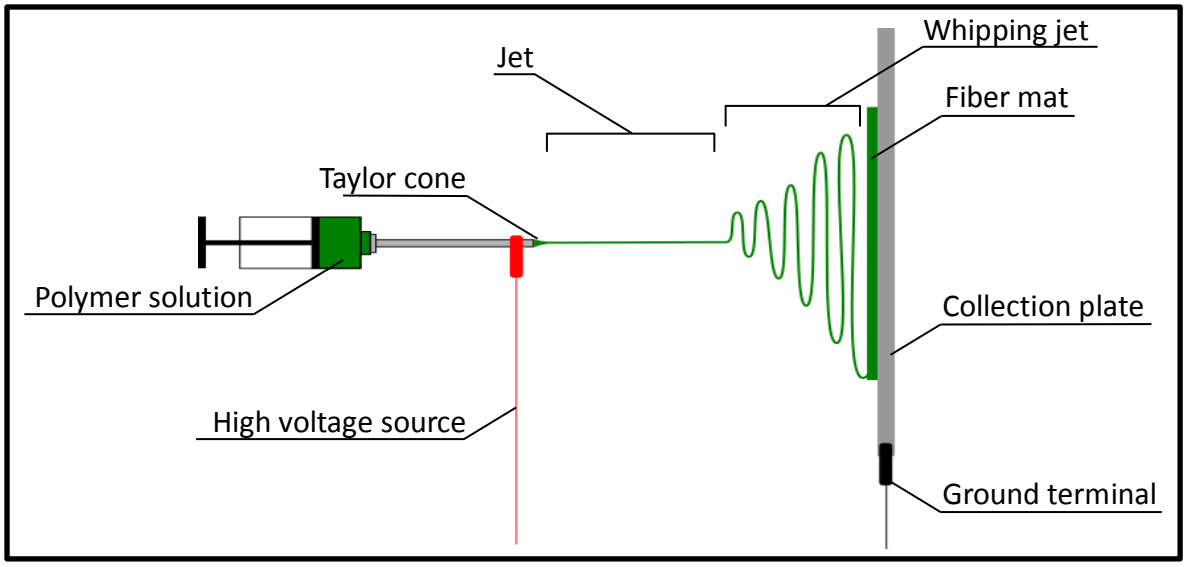

Figure 2: Electrospinning schematic. An overview of the electrospinning process with stages of the fiber jet labelled.

The unique nano-fibrous mat produced by electrospinning has several advantages over other scaffold fabrication techniques. Compared to other porous scaffolds, a nano-fibrous mat has an entirely interconnected pore structure created by the void space between fibers[23]. The geometry of a nano-fibrous mat also leads to a high surface area to volume ratio, which provides more surface area for cellular attachment to the material than porous scaffolds fabricated by other methods. Due to the high surface area to volume ratio, electrospun scaffolds have relatively high porosities[23]. A nano fibrous mat also mimics the geometry of native ECM, which is also made up of a network of nanometer scale fibers (proteins and glycosaminoglycans), thereby modelling the tissue microenvironment [23].

To determine which electrospinning parameters are most important for our fabrication process, the basic theory behind electrospinning must be understood. The formation of the fiber goes through several steps to transform from solution to dry polymer mat, through the use of a high powered electric field. The polymer jet goes through four main regions from extrusion to mat: the base, the jet, the whipping jet, and the collection[24]. The base refers to the region where the polymer is first extruded and where the solution is charged by the collector [24]. This base then experiences narrowing to the much thinner jet as the voltage differential accelerates the molecules within the solution. This narrowing occurs as a Taylor cone and the morphology and diameter of the cone is critical to the formation of reproducible and consistent

fibers[21]. Taylor cones are influenced by the combination of capillary and electrostatic forces which correlate to the pressure differential and charge differential on the fluid[25]. In practice, the electrostatic forces and the pressure differential are controlled by three electrospinning parameters: flow rate out of the syringe, viscosity of the solution, and the applied voltage[21]. Poor control of these parameters can lead to the instability in the Taylor cone or intermittent jet formation. Over a short distance, the jet becomes unstable as the free charge of the polymer jet and the ambient electric field lead to instabilities in the region known as the "whipping jet" stage in which the jet whips rapidly in x and y directions[20,26]. The final stage, collection, is the point at which the whipping jet is physically stopped by the collector. The placement of the collector therefore must be within the range of the whipping jet region to collect fibers[20].

The parameters critical to modifying the Taylor cone and achieving consistent fiber diameter and morphology are: viscosity (controlled by polymer concentration), material feed rate (controlled by flow rate), and electric field strength (controlled by voltage). Viscosity is key to the formation of uniform diameter fibers that do not exhibit beading. At very low polymer concentrations, beading and droplet formation is common, but at very high concentrations the droplet can dry out while still in the syringe tip[20]. The feed rate is directly correlated to fiber diameter; higher feed rates correlate to larger fiber diameters, but the electric field strength must be made strong enough to form a stable Taylor cone without dripping, but not so high that electrospraying occurs[23,25]. Therefore, In order to successfully electrospin cuffs, the electrospinning parameters must first be optimized.

Electrospinning is not the only method for fabricating these nanofibers, but it has certain advantages that make it the best choice for fabricating cuffs. Compared to other nanofiber fabrication methods, electrospinning is attractive for its versatility and relative simplicity[27]. The equipment required to create an electrospinning set up is minimal, the only major components are a syringe pump, high voltage power supply, and a collector[21]. The collection of the fibers is also not limited to a singular geometry; fibers have been successfully collected on flat sheets, cylindrical mandrels, and liquid baths among others[20].

2.3.2 Electrospinning for vascular grafts

Due to the advantages afforded by the electrospinning process, electrospinning has been studied for fabricating a small diameter vascular graft using a variety of polymers, both natural and synthetic. For vascular engineering, the focus has been on biocompatible polymers that have the structural integrity and elasticity necessary for vascular implants while still promoting endothelial and smooth muscle cell growth[28]. One common group of materials used are polyesters, for their degradability and mechanical properties, including PET (Dacron)[29], PCL (and PCL blends)[3,30-32], and PLLA[33]. Polyurethanes are also very common, but they are non-degradable[34-37]. Due to the ease of electrospinning the material, as well as the long history of FDA approval for implantation (used as the suture Monocryl since the 1980s[38]), we elected to use PCL or a PCL blend for the development of our vascular tissue scaffold.

2.4 Cuff material choice

2.4.1 Natural and synthetic blends

Natural material and synthetic polymers are both compatible with electrospinning, but often they are not suited to the intended application when used alone. Natural biopolymers are often used to mimic native ECM, to provide an environment similar to the *in vivo* environment[39,40]. Synthetic polymers generally have greater mechanical strength, which makes the materials much easier to manipulate. We have chosen to combine the advantages of these two types of materials by creating a blend of a synthetic polymer, PCL, and a natural material, gelatin.

2.4.1.1 PCL

The physical properties of PCL make it the ideal candidate as a base for electrospun cuff materials. It is an FDA approved polymer for several biomedical applications, most notably for drug delivery and as a suture material[38]. As discussed previously, PCL is highly compatible with electrospinning and has been used successfully for vascular applications in the past. Lee et al found that PLGA and PLA electrospun meshes collapse completely under comparable blood vessel physiologic loads, but that PCL and PCL blends have much higher tensile strengths and elastic moduli similar to native coronary artery[41]. However, despite PCL's favorable mechanical properties, the inherent hydrophobicity and lack of cellular binding sites lead to poor cellular

attachment to the material and make it difficult to use without modifying it in some way, often chemical modification of the surface of the material through plasma treating, or coating with a biological polymer[38]. Therefore, in order to improve integration of SMCs with the material, we have incorporated a biological material, gelatin, to help increase cellular attachment.

2.4.1.2 Gelatin

In order to increase cellular adhesion to PCL cuffs, we included gelatin in the cuff material. Gelatin, a heat denatured form of collagen, has been shown to improve vascular smooth muscle cell attachment to electrospun PCL meshes in other applications[3,31,32,42]. When collagen is denatured to form gelatin, RGD peptide motifs are exposed providing sites for cell attachment, leading to greatly improved cell attachment to gelatin over PCL[43]. Gelatin is also a more hydrophilic material than PCL, so incorporation of gelatin can further improve cell attachment by decreasing hydrophobicity[38]. However, gelatin has a far lower mechanical strength than PCL[3].

2.4.2 Coating and co-spinning

Although both gelatin and PCL must be present in the cuff scaffold materials, there are several methods that could be used to blend the two materials. Two common methods to incorporate natural biopolymers are to coat the electrospun PCL scaffold, or to create blended fibers by co-spinning with both materials[38]. Gelatin has been incorporated with PCL by both of these methods [3,44,45 41 31,46 47]. However, there has not been a direct comparison of the effectiveness of the two methods. Here we compared the effectiveness of these two gelatin incorporation methods to each other and to pure, unblended PCL. Figure 3 shows an overview of these three experimental groups, the differences in gelatin content and how gelatin is incorporated into the materials.

2.4.2.1 Co-spinning

Due to the highly blendable nature of PCL and the ease with which different polymers can be blended in electrospinning solvents, there is a large body of work in creating blended "co-spun" fibers. Collagen, and its denatured form, gelatin, have been cospun with PCL in order

to improve cellular attachment and wettability of the electrospun PCL fibers[3,44,45]. However, this process can lead to a decrease in mechanical strength and extensibility compared to pure PCL fibers[41].

2.4.2.2 Coating

Coating allows for the incorporation of gelatin onto the surface of the PCL material through a post processing step after electrospinning. Due to the poor ability of cells to adhere to pure PCL, coatings of biological proteins such as laminin, fibronectin, and gelatin have been used to improve attachment[31,46]. However, direct adsorption of gelatin onto PCL scaffolds is transient; a brief saline wash is sufficient to remove the gelatin from the PCL surface[47]. Certain methods can increase the stability of gelatin coating, such as physical entrapment, chemical crosslinking, or chemically bonding gelatin to the PCL scaffold[32,47]. We chose to use chemical crosslinking to stabilize gelatin coating for the ease of the procedure and for the fact that it does not modify the underlying PCL fibers. Therefore, gelatin can be stably incorporated onto PCL fibers without affecting the underlying PCL material allowing for a direct comparison of coating and cospinning of gelatin.

Genipin is a natural crosslinking agent that can be used to crosslink gelatin coatings[48]. Genipin has the ability to crosslink proteins with primary amine groups, which stiffens the gelatin[49]. By crosslinking the gelatin with genipin, the gelatin coated onto the fibers can be made less susceptible to gelatin desorption[48]. Since genipin crosslinking is dependent on amine groups, this crosslinking agent should not have any effect on the underlying PCL material, which does not contain the necessary amine groups.

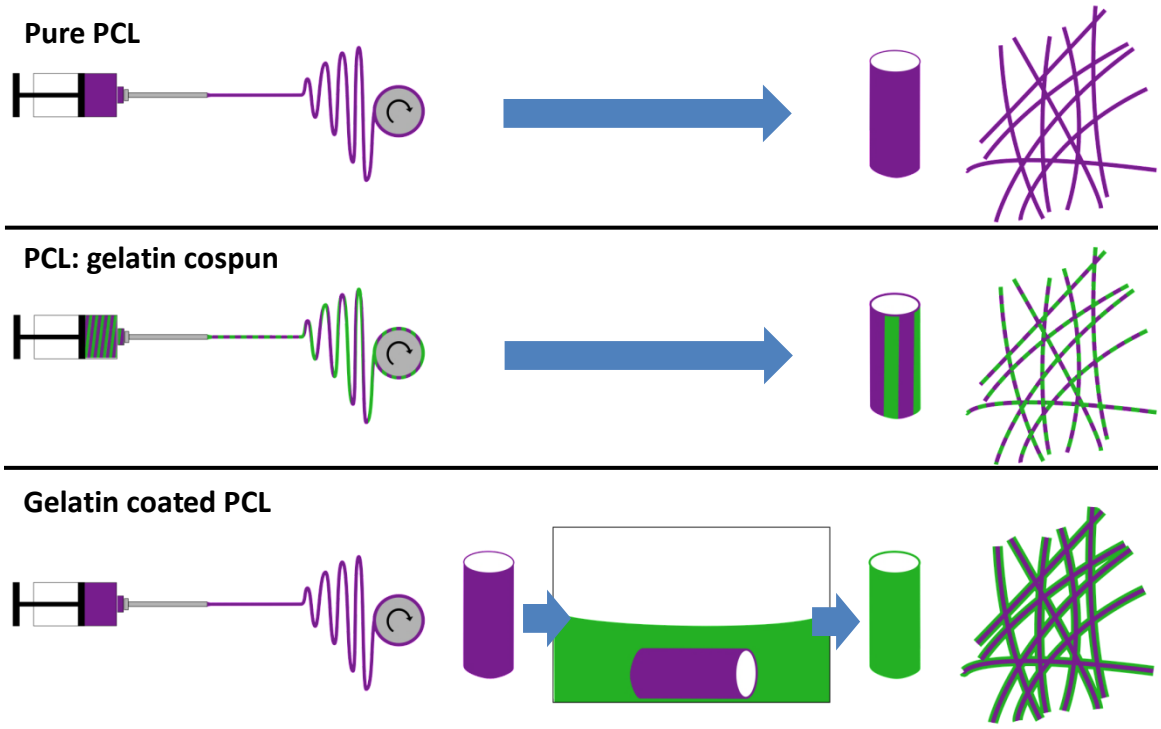

Figure 3: Gelatin incorporation methods for fabricating blended cuffs. Cartoons for the production of experimental cuffs. **Top:** Pure PCL cuffs are fabricated by electrospinning PCL onto spinning mandrel. **Middle:** PCL: gelatin cospun cuffs are fabricated by electrospinning gelatin and PCL dissolved in the solvent solution to make blended fibers. **Bottom:** Gelatin coated PCL cuffs are fabricated by electrospinning Pure PCL cuffs that are placed in a gelatin coating bath creating pure PCL fibers with a layer of gelatin on the surface.

2.5 Cuff evaluation methods

2.5.1 Electrospun morphology: Porosity, pore size and fiber diameter

Porosity is a critical component to successful cellular infiltration into a scaffold. Porosity is defined as the void volume of the scaffold relative to the entire scaffold volume. The high surface area to volume ratio of electrospun scaffolds allows for relatively high porosities to be achieved[23]. Vascular smooth muscle cell seeding in particular has been found to be optimal in scaffolds with 75%-90% void fraction[2]. At these high porosities, vascular smooth muscle cells can infiltrate and grow into the material. Void fractions of this range are common in electrospun materials, and were therefore the target for electrospun cuffs[20].

Appropriate pore size is also a critical feature for cellular infiltration into the material. It has been shown that smooth muscle cell infiltration into scaffolds is greatest in the size range of 63–150μm for salt leached PLLA scaffolds[2]. However, due to the inherently small pore sizes

of electrospun scaffolds, it is unlikely we will be able to achieve pore sizes in this range for a blended PCL and gelatin material[45]. Though pore sizes for electrospun PCL composites have been reported to range from sub-micron pore sizes to 100µm, it is entirely dependent on fiber diameter, and the use of separate pore inducing techniques such as salt leaching[50]. For nanofibrous mats, pore sizes are often too small to support cellular infiltration[38]. However, it has been found that some infiltration can occur with pore sizes over 10µm, and this is within the range for electrospun materials, and was thus used as the target for pore size in the present study[1].

Due to the fibrous nature of an electrospun mat, measuring pore size directly is difficult, as distinct pores do not exist in a fibrous mat. Pore size is directly correlated to fiber diameter, and by the packing efficiency of the fibers in the material[51]. Therefore, in order to modulate pore size, the fiber diameter of the scaffold must be manipulated. As discussed earlier, the parameters of the electrospinning processes are the determining factor in fiber diameter, and therefore by optimizing the electrospinning parameters for the formation of the largest possible fibers, pore size can also be maximized. Using a model based on the empirical fiber diameter and porosity of the scaffold, we can estimate pore size as:

$$\langle r \rangle \cong \frac{\omega}{\ln\left(1/\varepsilon\right)}$$

Where <r> is the theoretical pore radius, ω is the fiber diameter, and ε is the porosity[52]. From this theoretical pore size, we can predict the amount of cellular infiltration that will occur.

2.5.2 Mechanical properties

The mechanical properties are an important feature of cuffs, and one that will likely be impacted by the different methods of gelatin incorporation. As described previously, creating cospun fibers of PCL and a natural protein like gelatin can significantly decrease overall strength and extensibility, while a gelatin coating is less likely to impact these properties. For the design of cuffs, we are mainly concerned that they have adequate mechanical strength, and minimal compliance mismatch between the material and tissue. To measure the mechanical properties of these materials, we used a tensile pull to failure test modified from the procedure used to test cell derived tissue rings[7]. Briefly, a single cuff was uniaxially pulled to failure

circumferentially and ultimate strength and maximum load was measured and compared to reported values for smooth muscle cell rings and segments of native arterial tissue[53-55].

Ring tensile testing does not provide direct information about compliance, so it cannot be used to asses compliance directly[54]; however there are other parameters that relate stress and strain that can be collected from uniaxial tensile testing. Elastic modulus has been used to evaluate the "stiffness" of TEBV from ring tensile testing[55], and it has been shown that for large deformations, 25%-80% of failure load, the modulus measured by ring tensile tests is comparable to the modulus measured via pressurization of a tube[54]. As this parameter can also measure "stiffness" in the cell derived ring constructs, this method seems adequate for evaluating similarities in stiffness between cell derived tissue and cuff materials.

2.5.3 Attachment of SMC to cuff materials

As discussed above, one of the greatest benefits afforded by incorporating gelatin into PCL constructs is improved cell attachment[56]. This will likely also impact the degree of cuff integration with cell derived rings, as smooth muscle cells must attach and grow out onto the material for successful integration. A metabolic assay, based on reduction of AlamarBlue® dye, has been shown to be able to detect the percent attachment of cells to electrospun scaffolds therefore we chose to use this method to compare our PCL and gelatin composite materials[57].

2.5.4 Outgrowth of SMC over cuff materials

Outgrowth is also a key component of cuff integration with cell derived tissue. Outgrowth of cells onto the surface of the material makes up for a large portion of tissue cuff integration. Outgrowth provides us with a combined measurement of cellular proliferation and migration of cells on the material. As with attachment, gelatin incorporation will provide more cell recognition sites on the material and will likely affect the rate at which cells can grow out from a single location onto the surface of the material. By seeding a high density droplet of cells onto a thin electrospun film, outgrowth distance can be measured and the rate of outgrowth can be calculated[46].

2.5.5 Cuff tissue integration

Cuff tissue integration can be measured directly through fusion of PCL and gelatin PCL composite cuffs with engineered tissue. To measure the strength of the bond between tissue and cuffs, longitudinal pull to failure testing can be used to reveal not only failure strength but also the location of tissue failure. This testing is required by ISO standards for the evaluation of vascular graft materials, and has been used to evaluate the mechanical properties of native tissue[58-60]. Histological analysis of tissue constructs can be used to directly observe cellular integration by showing how cells interact with cuffs[13]. These tests allow for the direct comparison of PCL and gelatin PCL composite materials, and indicate which materials integrate best for use as cuffs.

Chapter 3. Fabricate and characterize cuff scaffold materials

3.1 Introduction

The goal of this aim was to establish methods for electrospinning PCL and gelatin PCL composite cuffs, and then evaluate the material properties of the cuffs. Two methods for incorporating gelatin into composite materials were developed and tested: PCL:gelatin cospinning and gelatin coating of PCL. These two PCL and gelatin composites, and pure PCL materials, were then compared to determine the differences in scaffold morphology (fiber diameter, porosity, and pore size) and mechanical properties. These differences revealed the impact of different gelatin incorporation methods on cuff materials, and the feasibility of using these composite materials as cuffs for SMC tissue tubes.

3.2 Methods

3.2.1 Fabrication methods

3.2.1.1 Electrospinning set up

Electrospinning was performed using the apparatus in Dr. Anjana Jain's laboratory in the Department of Biomedical Engineering at WPI. A motor with variable speed (2Z846, Grainger), and syringe pump (SP200i, World Precision instruments), were placed within a custom acrylic container. A 3mL syringe (BD Falcon, Fischer Scientific, 14-823-40) loaded with polymer solution was attached to an 18-gauge blunt ended needle, and loaded into the syringe pump. The positive terminal of a high voltage power supply was attached to the needle via alligator clips and the ground terminal was attached to the frame of the motor. The collecting mandrel was attached to the motor using a series of couples. A custom 9mm to 5/8" couple was machined at the Higgins Lab Machine Shop from a clamp-on rigid shaft couple with machinable bore (McMaster Carr, 3084K32), one end of which was drilled to 9mm in diameter using a lathe to accommodate the 2mm mandrel couple. This couple was connected to a 9mm outer diameter and 2mm inner diameter couple (A 5X 9M0204, SDP) attached to the collector mandrel (2mm stainless steel hypo tube, ASIN B000FMYN92, Amazon Supply (formerly

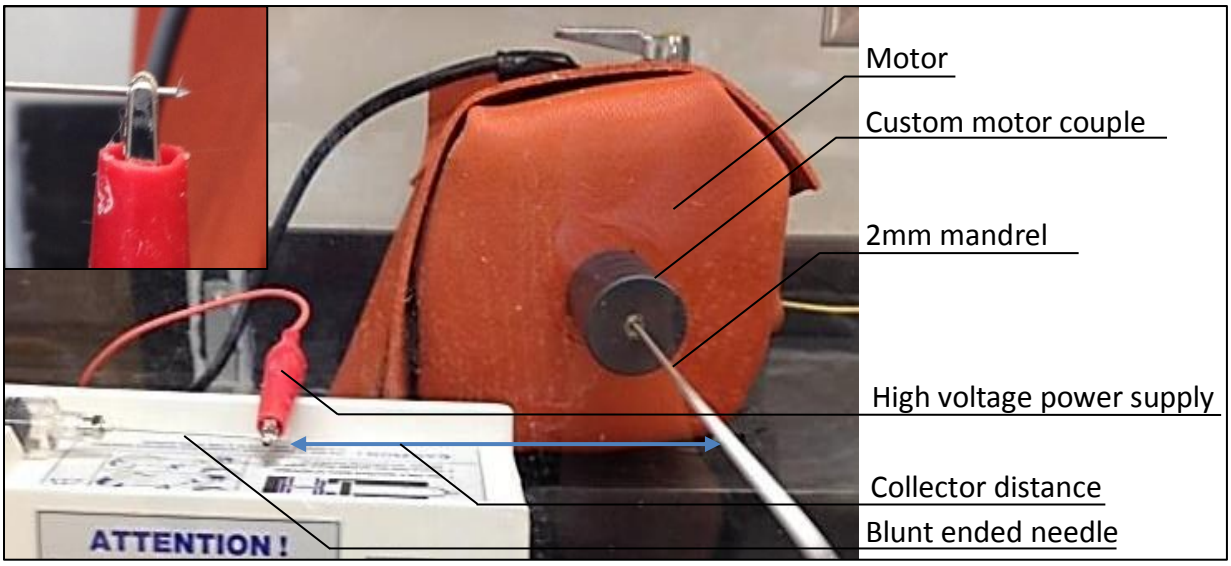

Figure 4: Electrospinning setup. Major components of the set up are labeled above, blue arrow indicates collector distance (10cm) Inset: image of Taylor cone formed at syringe tip while electrospinning pure PCL fibers.

SmallParts Inc.) cut to 6 inches in length). A photograph of the electrospinning system is shown in Figure 4.

Polymer solutions were made of poly-ε-caprolactone (PCL; 440744, Sigma Aldrich) and 300 bloom gelatin from porcine skin (G2500, Sigma Aldrich) dissolved in 2,2,2 Tri-fluoro-ethanol (TFE) (T63002, Sigma Aldrich) at 12% weight/volume and mixed overnight on a stir plate. For blended PCL:gelatin solutions, gelatin and PCL are dissolved separately into TFE at 12% weight/volume and mixed at either a 50:50 ratio or an 85:15 ratio, to which a small volume of glacial acetic acid (3µl/mL) was added to aid in the miscibility of PCL and gelatin[61]. The 50:50 ratio blends were used in optimization testing, and 85:15 ratio samples were used for all further cuff fabrication so that the final concentration of gelatin in cospun samples and gelatin coated samples was always 15%.

3.2.1.2 Electrospinning optimization

In order to ensure both a stable Taylor cone and to maximize the fiber diameter, the electrospinning parameters were optimized using a 50:50 blend of PCL:gelatin and the parameters listed in Table 2. For cuff fabrication, pure PCL samples and 85:15 PCL:gelatin cospun samples were both electrospun at the following parameters: 15cm collector distance,

flow rate of 5mL/hr., voltage of 20kV, spin time of 12 minutes, and a rotational speed of 265rpm as measured with Neiko 20713A laser photo tachometer.

Table 2: Parameter ranges for electrospinning optimization. Collector distance, electric field strength, and flow rate ranges chosen for optimization. All 24 combinations of the settings below were tested.

Collector distance	10cm
	15cm
Electric Field Strength	12kV
	15kV
	17kV
	20kV
Flow Rate	2mL/hr.
	3mL/hr.
	5mL/hr.

3.2.1.3 Gelatin coating optimization

To create a stable gelatin coating, we adapted the genipin crosslinking method reported by Zhang et al for coating salt leached PCL scaffolds with gelatin[48]. Cuff samples of pure PCL were electrospun as described above. Gelatin from porcine skin (300 bloom; G2500, Sigma Aldrich) was dissolved in deionized water at 37°C at either 5.0% or 0.5% weight by volume with 0.02% weight by volume of genipin (G4796, Sigma Aldrich). The gelatin solution and cuff samples were placed into the lower 50mL conical tube of a SteriFlip filtration system (SC50FL025 Fischer Scientific) in a 37°C water bath and a vacuum was applied for 30 minutes to draw gelatin into the pores. Cuff samples were removed from gelatin solution and placed in an oven at 37°C for 8 hours to facilitate genipin crosslinking. Saturated glycine (G7126, Sigma Aldrich) solution was added to samples to halt the crosslinking reaction, and samples were submerged in 0.1M NaH_2PO4 (S5136, Sigma Aldrich) pH 9.1, to neutralize them. Samples were rinsed extensively in DI water and allowed to air dry overnight before further testing. An overview of the procedure is shown in Figure 5.

Images of PCL cuff samples coated with 0.5% or 5.0% gelatin solution were acquired via SEM as described below, and the gelatin content was determined by measuring the weight of samples before and after the coating process.

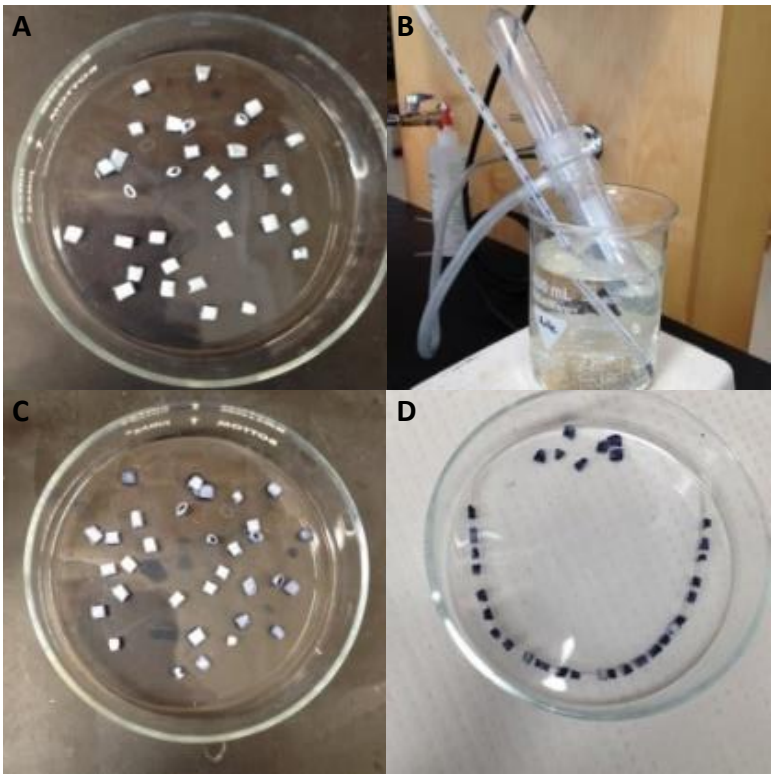

Figure 5: Gelatin coating process. A) Pure PCL cuffs before coating **B)** SteriFlip vacuum system loaded with PCL cuffs in 5% gelatin and 0.02% genipin in 37°C water bath. **C)** Gelatin coated cuffs directly after removal from coating solution. **D)** Gelatin coated cuffs after crosslinking incubation and air drying, note that blue genipin coloring was only observed in 5% gelatin coated samples.

3.2.1.4 Electrospinning flat sheets

Electrospinning was performed as described above, with the only change being the collector geometry and spin time to spin flat sheets of material as opposed to cylindrical cuff materials. In place of the 2mm stainless steel mandrel, a large custom aluminum drum was attached to the motor and wrapped with an aluminum sheet. The spin time was also reduced to 6 minutes instead of the 12 minutes used for spinning on 2mm mandrel. The aluminum sheet was removed and laid flat and approximately 3cm X 3cm samples of material were cut with a scalpel. To coat samples, cut samples were glued at the corners using silicone medical adhesive to a 22 X 40mm glass coverslips to prevent samples from folding and floating while submerged. The coating process was then performed as described above using 0.5% gelatin and 0.02% genipin, placing coverslips with material directly into gelatin solution in SteriFlip vacuum chamber. Samples were removed from coverslips before use.

3.2.2 Characterization methods

3.2.2.1 Scanning electron microscopy

SEM imaging was performed on a JSM 7000F electron microscope in the mechanical engineering department at WPI to visualize electrospun samples and assess fiber diameter. A low accelerating voltage (2kV) and low current (1mA) were used to prevent damage to samples. A 12mm working distance and a range of magnifications from 1,000X to 10,000X were used as indicated on individual figures. For analysis of fiber diameter 10,000X micrographs were used.

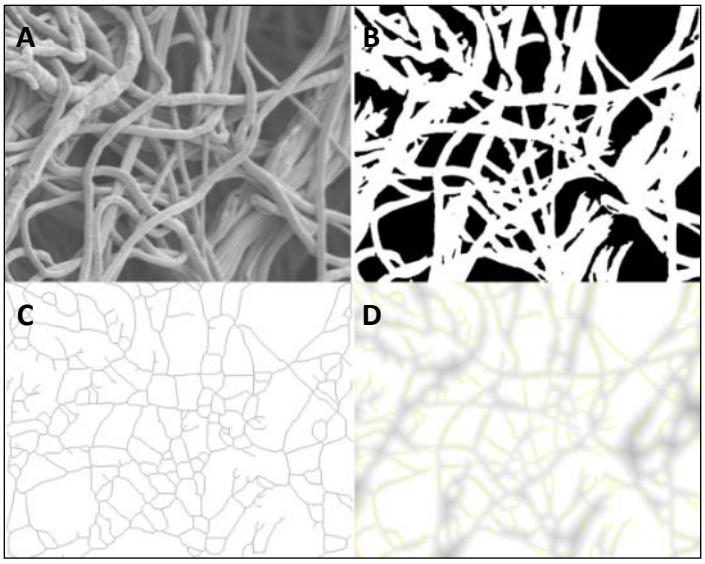

Figure 6: DiameterJ fiber diameter measurements. A) Raw SEM image of Pure PCL fibers **B)** binarized fiber image **C)** Fiber axis map of all fibers detected in image **D)** Locations used for fiber diameter measurements highlighted in yellow.

3.2.2.2 Gelatin visualization

Coomassie Brilliant blue dye was used to visualize gelatin content in cuff materials. Two flat sheet material samples, fabricated as described above, of each cuff material were placed in Bradford Assay reagent (B6916 Sigma) for 10 minutes. Following this, unbound dye was washed off in running deionized water for 10 minutes.

3.2.2.3 Measuring fiber diameter

DiamaterJ, an ImageJ plugin developed by the National Institutes of Standards and Technologies (NIST), was used to make several thousand measurements of fiber diameter on each SEM micrograph. A full description of DiameterJ is given by Hotaling et al[62]. Briefly, one of 16 algorithms is used to binarize SEM images yielding white fibers and black background. The DiameterJ plugin identifies and maps all fibers visible in the image and measures the diameters along all lengths of fibers not located at fiber intersections. This process can be seen in Figure 6 on a representative SEM image. A minimum of 3 regions were analyzed within one cuff segment of each material type.

3.2.2.4 Porosity measurements

We used the liquid intrusion method, also known as the liquid displacement method, to measure porosity, a method commonly used for estimating porosity in electrospun materials. Based on the methods described by Soliman et al[52], approximately 20mg samples of cuff materials were weighed on an analytical balance, and based on the gelatin content; the volume was calculated from the density of PCL, 1.145g/mL, and the density of gelatin, 1.3 g/mL. Samples were then soaked overnight in 100% ethanol, and weighed again. Using the density of ethanol, 0.789g/mL, the volume of ethanol was calculated. Porosity is reported as volume of ethanol as a percentage of the total volume of the scaffold. 3 samples of cuff material for each group were analyzed (n=3) and compared using a one way ANOVA with Tukey post-hoc comparison tests.

3.2.2.5 Theoretical pore size modeling

The average pore size for scaffolds was determined using a theoretical model described in Chapter 2[52]. Average pore size was defined as:

$$\langle r \rangle \cong \frac{\omega}{\ln\left({}^{1}/_{\varepsilon}\right)}$$

Where ω was the average fiber diameter determined from SEM imaging, and ε is the porosity determined by ethanol intrusion.

3.2.2.6 Tensile testing of electrospun cuff materials

Introducing biological proteins via co-spinning is known to affect the mechanical properties of electrospun scaffolds, therefore tensile pull to failure testing was used to compare cuff materials and determine the effects of incorporation of gelatin via coating or co-spinning[41]. cuffs were tested using methods established for tensile testing ring shaped segments of blood vessel and for testing cell derived ring constructs[54,55]. Materials were prepared as described previously and ten approximately 4mm long samples were fabricated for each experimental group: pure PCL, PCL:gelatin cospun, and gelatin-coated PCL. The dimensions of these segments were measured using calipers and samples were wetted in a phosphate-buffered saline solution for 30 minutes prior to testing. These segments were placed on custom wire grips and the initial

distance between grips was measured using calipers. Samples were pulled to failure at a rate of 10mm/min in an Instron ElectroPuls E1000. The resulting load and extension data were then analyzed in MatLab to determine the ultimate tensile strength (UTS), elastic modulus, and extensibility of each sample. 10 cuff samples were analyzed (n=10) and compared using a one way ANOVA with Tukey post-hoc comparison tests.

3.3 Results

3.3.1 Electrospinning optimization

To determine the effects of varying the electrospinning parameters, 24 combinations of settings were evaluated for successful and consistent Taylor cone formation. Table 3 summarizes the results and highlights the most successful combinations of settings. It was shown that increasing the flow rate required an increase in voltage to maintain the Taylor cone. As collector distance was increased, voltage also must be increased to maintain the Taylor cone.

Table 3: Taylor cone optimization. Taylor cone formation and fiber collection results from varying electrospinning parameters. Grayed out cells indicate suboptimal Taylor cone formation. White cells indicate successful fiber collection. Black box indicates combination of parameters selected for subsequent cuff fabrication.

Collector distance 10cm					Collector distance 15cm				
	Voltage					Voltage			
Flow	**12kV**	**15kV**	**17kV**	**20kV**	**Flow**	**12kV**	**15kV**	**17kV**	**20kV**
2mL/hr.	works well, stable cone	flickering cone/stream	multiple streams that dried out, flickering cone	no visible cone flickering stream	**2mL/hr.**	Dripping, no cone, no fibers collected	some dripping, otherwise stable cone	flickering cone, barely visible, multiple streams	great deal of flickering cone not visible
3mL/hr.	dripping with cone visible, no fibers collected	works well stable cone very occasional flickering	moderate, flickering but not excessive	no visible cone flickering stream	**3mL/hr.**	Dripping, no cone, no fibers collected	Dripping occasional stream, no fibers collected	works well, steady cone, no flickering	flickering cone multiple streams
5ml/hr.	dripping, no cone, no fibers collected	beading initially, very long cone, stable but beginning to dry out	works well, steady cone	cone formed on drip, multiple streams	**5ml/hr.**	Dripping, no cone, no fibers collected	Dripping occasional stream, no fibers collected	Dripping occasional stream, no fibers collected	works well stable cone very occasional flickering

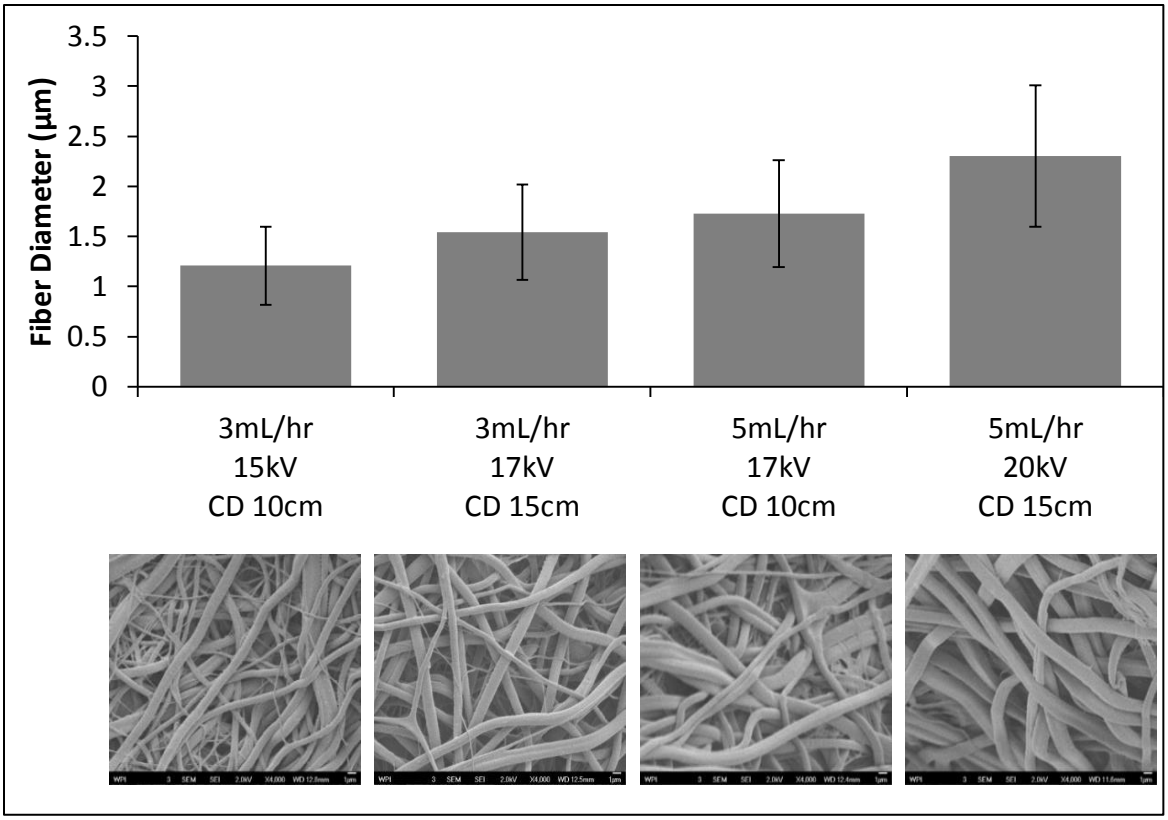

Figure 7: Fiber diameter parameter screening. Average ± standard deviation of fiber diameter for parameter combinations leading to successful fiber formation. Representative SEM micrographs of fibers at 10,000X magnification are pictured below sample labels. At least 16468 fiber measurements were obtained from a minimum of 3 micrographs per sample (n=1 sample per group).

From parameter settings that successfully formed a Taylor cone, the fiber diameter was measured, and these data are summarized in Figure 7. From these samples, it appeared that higher flow rates and voltages resulted in larger fiber diameters. Using these data, it was determined that for all sample fabrication for subsequent studies, a flow rate of 5 ml/hr., voltage of 20kV, and collector distance of 15cm would be used as it led to successful Taylor cone formation and the largest fiber diameters.

The gelatin coating process was also optimized to determine the appropriate amount of gelatin to use to coat samples based on SEM imaging and gelatin content by weight. Initially 5% gelatin coating solution was used, based data from Zhang et al[48]. However, this resulted in a final concentration of gelatin in cuffs of 82.4%. SEM images, shown in Figure 8, showed that the PCL fibers were completely obscured by gelatin at this high concentration. For this reason,

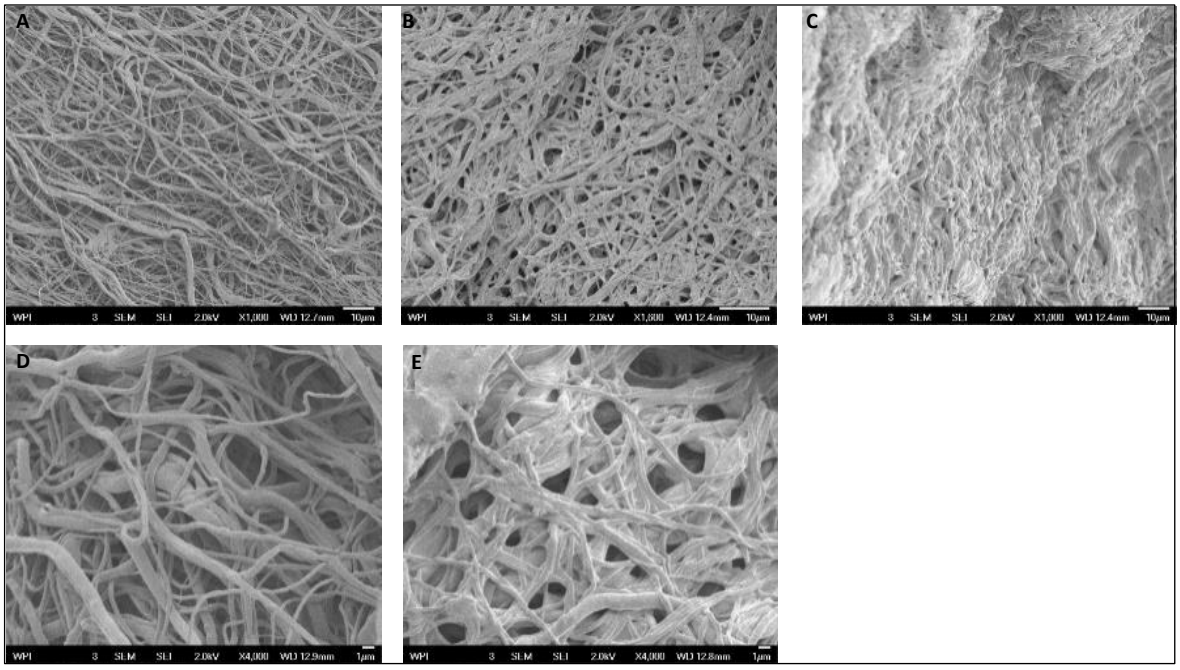

Figure 8: Gelatin coating optimization. SEM micrographs of uncoated pure PCL fibers, 0.5% gelatin solution coated, and 5% gelatin solution coated samples. Top row: 1,000X magnification of **A)** uncoated fibers **B)** 0.5% gelatin coated fibers and **C)** 5% gelatin coated fibers. Bottom row: 4,000X magnification of **D)** uncoated fibers and **E)** 0.5% gelatin coated fibers. Due to the density of the gelatin coating obscuring the fibers in the material, images of 5% gelatin coated materials could not be obtained at 4,000X magnification.

the gelatin solution was decreased to 0.5%, which yielded a 15% final gelatin content by mass, and individual PCL fibers were still visible via SEM imaging. In order to maintain the same gelatin concentration in cospun PCL:gelatin samples as the gelatin-coated PCL samples, the ratio of PCL to gelatin in the solvent solution was chosen to be 85:15, PCL: gelatin.

3.3.2 Fiber diameter

Using the parameters determined from the optimization study, cuffs were spun of the three sample groups: pure PCL fibers, PCL:gelatin cospun fibers, and gelatin-coated PCL fibers. Figure 9 shows histograms of fiber diameter distributions along with representative images of samples at 10,000X magnification. Pure PCL materials had fibers with an average diameter of 536µm ±.365µm. Cospun PCL:gelatin materials were found to have a smaller diameter with an average of only 267µm±.173µm. Gelatin-coated PCL fibers appear to have an increased fiber diameter compared to pure PCL fibers, on average 670µm±.204µm, as the gelatin coating

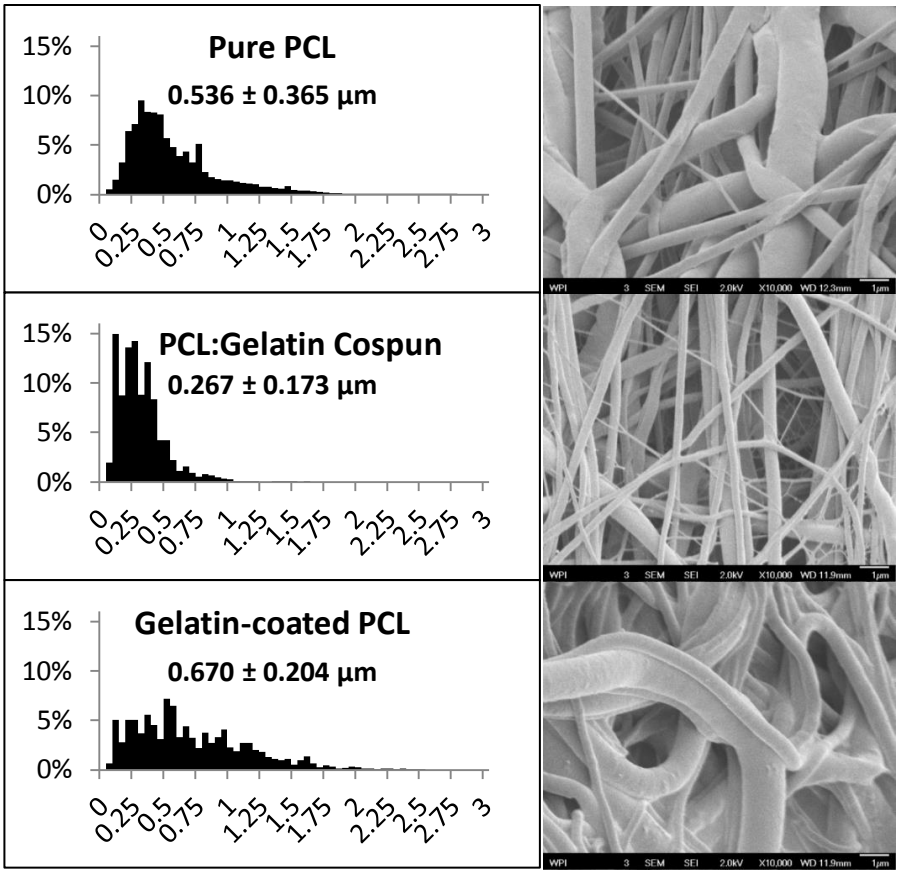

Figure 9: Fiber diameter of PCL and PCL gelatin composites. Fiber diameter distributions computed by DiameterJ are shown on the left and representative micrographs of each material at 10,00X magnification are shown on the right. n ≥ 15036 fiber measurements, from a minimum of 3 micrographs per sample, (n=1 sample per group).

increases fiber diameter. The gelatin coated fibers appear to have a much wider distribution of fiber diameters than either of the other samples.

3.3.3 Pore size and porosity

The porosity of the cuffs was measured using the ethanol intrusion method. Porosity, reported as void fraction, can be seen in Figure 10. Pure PCL had the largest void fraction (83.5%±0.3%), followed by the gelatin-coated PCL at 78.5% ± 5.4%, and lowest was the PCL:gelatin cospun material at 73.6% ±1.0%. The porosity of the pure PCL samples was significantly greater than the PCL:gelatin cospun material, but neither group was significantly different from gelatin-coated PCL. Using the mean fiber diameter values and average porosity for each material, pore size was calculated. The summary of the theoretical pore size can be seen in Table 4. The overall trend was very similar to that of the porosity and fiber diameter, with the pore size of cospun materials being far lower than either pure PCL or gelatin-coated PCL fibers. Pure PCL fibers and gelatin-coated fibers have an average pore size between 5.5 and

6.0 µm in diameter compared to PCL:gelatin cospun samples with an average pore diameter of only 1.7µm.

Table 4: Theoretical pore size.

Sample	Fiber diameter (ω)	Porosity (ε)	Average pore diameter (2r)
Pure PCL	0.536	0.835	5.960
PCL:gelatin cospun	0.267	0.736	1.739
Gelatin-coated PCL	0.670	0.785	5.522

3.3.4 Gelatin visualization

A protein dye, Coomassie Brilliant Blue, was used to stain the gelatin in electrospun samples to visualize uniformity of gelatin integration. Staining revealed the presence of protein in PCL:gelatin co spun materials and gelatin-coated PCL materials. However there appeared to be some variability in gelatin content in gelatin-coated materials. Pure PCL fibers still retained some background dye. Figure 11 shows stained samples.

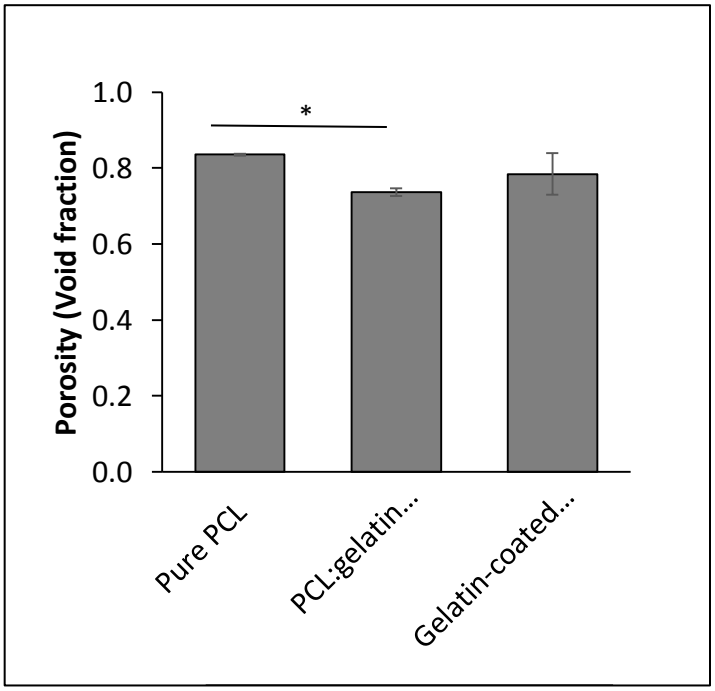

Figure 10: Porosity. Liquid intrusion porosity measured for all groups. * indicates statistically significant difference at $p<0.05$ level detected by one way ANOVA using post hoc Tukey comparisons n=3 samples

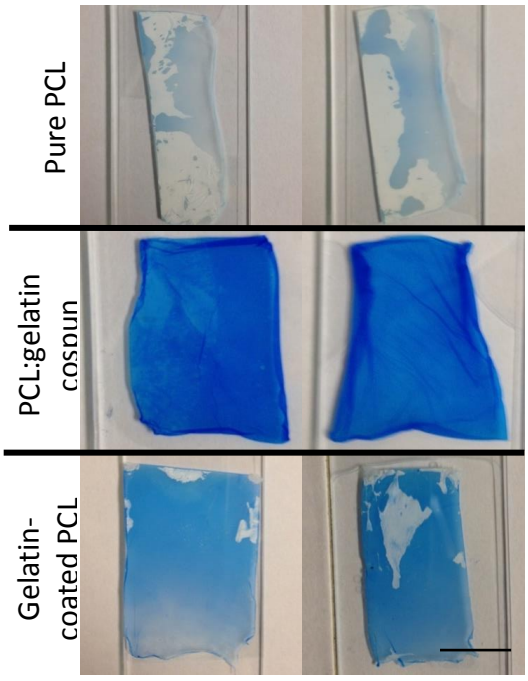

Figure 11: Gelatin visualization. Coomassie brilliant blue staining of pure PCL materials, PCL:gelatin cospun materials and gelatin-coated PCL materials scale bar 1cm.

3.3.5 Mechanical testing

The impact of coating and co-spinning of gelatin on the mechanical properties of the scaffolds were evaluated via ring mechanical testing. It was expected that by co-spinning with gelatin, the overall strength of the fibers will decrease, but that coating will have minimal impact on the mechanical properties of the scaffold. As seen in the representative stress strain curves, Figure 12, gelatin cospinning greatly decreased the mechanical strength, but gelatin coating did not. To quantify the differences in the mechanical properties the average UTS, strain at failure extension, the maximum load, and the linear elastic modulus were compared. These data are summarized in Figure 13. The intrinsic material strength did not appear to be impacted by the coating. The UTS (Figure 13A), is not significantly different between pure PCL and gelatin-coated PCL materials, but PCL:gelatin cospun samples were significantly less strong. However, based on maximum load, there appears to be a difference between coated and pure samples (Figure 13C). Coating and co-spinning both appear to have a significant impact on extensibility, reported as maximum strain, (Figure 13B). Both gelatin incorporation techniques decreased the maximum strain, with gelatin co-spinning resulting in significantly decreased failure strain compared to gelatin coating. The stiffness of the materials, reported as linear elastic modulus in Figure 13D, was also significantly increased by both gelatin incorporation methods.

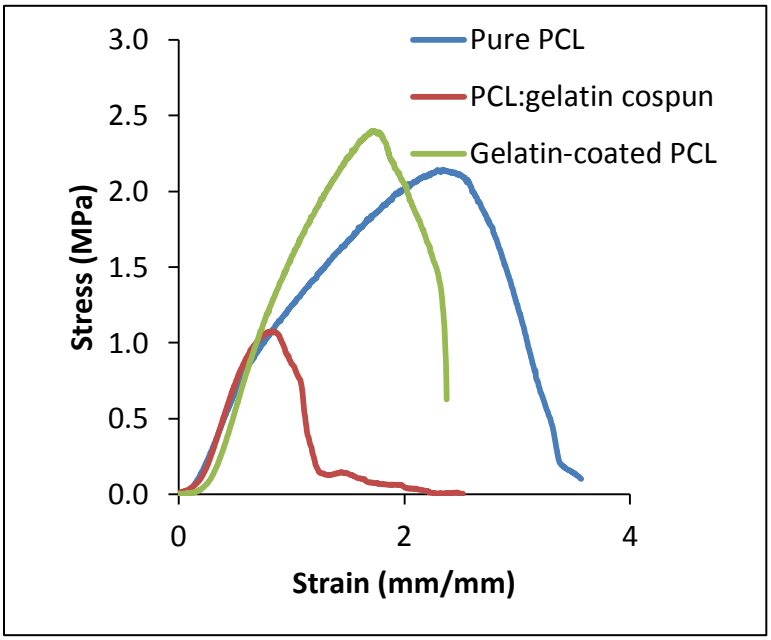

Figure 12: Representative stress strain curves. Individual samples of each material were chosen that most closely represent the average properties and stress and strain was plotted here.

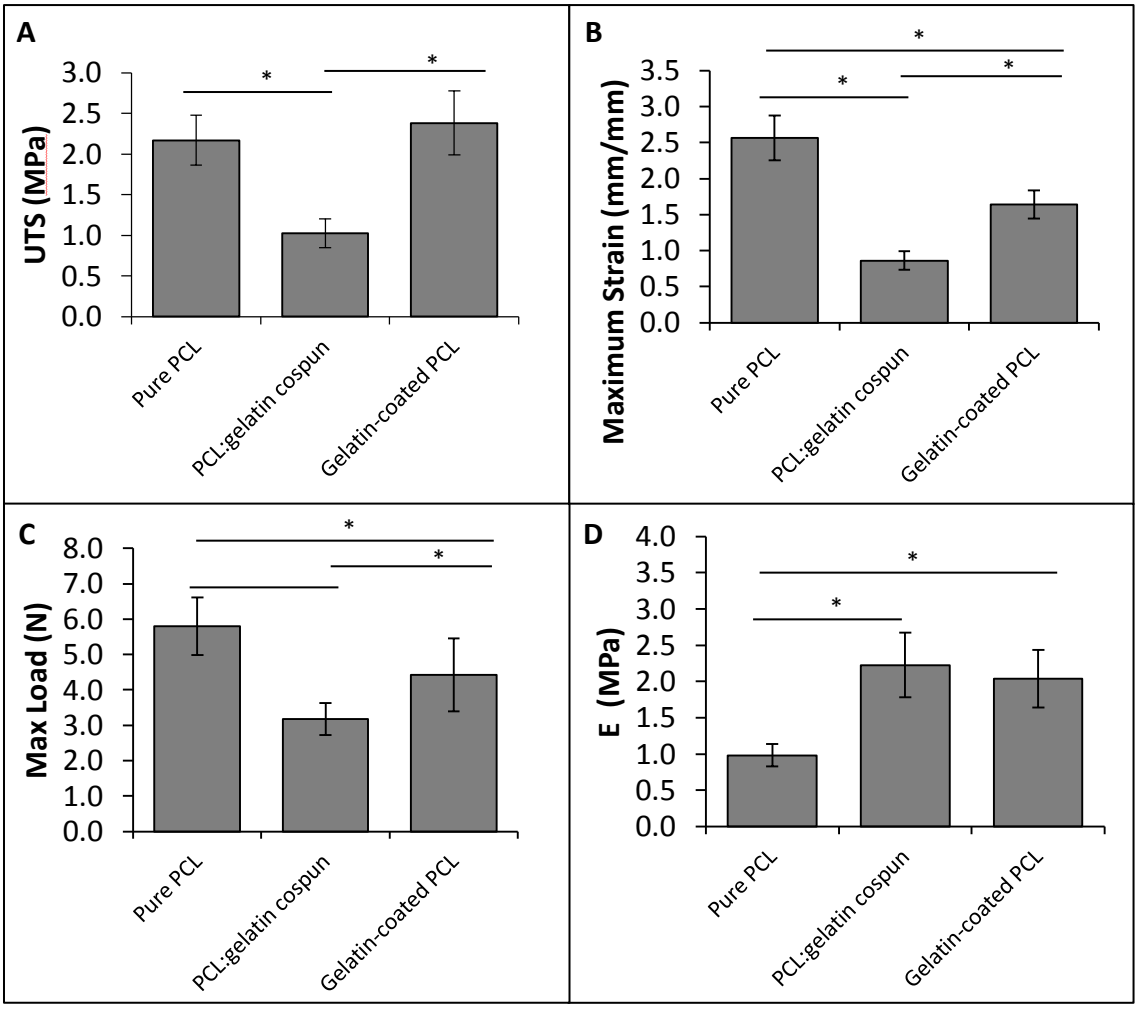

Figure 13: Mechanical properties. A) The ultimate tensile strength (UTS), **B)** the strain at the UTS (Max Strain),**C)** the maximum load (Max load) and **D)** the linear elastic modulus of cuffs determined through tensile pull to failure testing. * indicates statistically significant difference at $p<0.05$ level detected by one way ANOVA using post hoc Tukey comparisons n=10 cuff samples

3.4 Discussion

3.4.1 Fabrication optimization

The optimization of the protocol for cuff fabrication revealed the effects of several factors that impact electrospinning. From the parameter screening, it is clear that voltage and flow rate are closely linked in both successful Taylor cone formation and fiber diameter. It appears from our data, and from the findings of others [23], that increasing flow rate increases

fiber diameter, as can be seen in Figure 7. However, in order to maintain the flow rates, the voltage must be increased to form a stable Taylor cone, as can be seen in Table 3. Based on the fiber diameters of the two successful 5mL/hour spins, it appears that increasing the distance to the collector also increases the overall fiber diameter. However, based on the Taylor cone formation, these data indicate that increasing collector distance also requires increasing the voltage. By increasing the electric field strength, the increased electrostatic forces on the polymer jet are able to maintain a stable Taylor cone despite the increased gravitational forces caused by increasing the flow rate.

For gelatin coating optimization, it was critical that the nanofibrous structure not become completely obscured by the gelatin coating. A concentration of 5% gelatin was initially chosen based on the protocol used by Zhang et al[48]. However, the range of the pore sizes in our PCL materials are far smaller on average (<5.9µm) compared to the salt leached materials described, which had pore sizes ranging between 200µm and 300µm. This disparity in pore sizes caused the pores in our electrospun PCL to be completely obscured by the gelatin coating when 5% gelatin solution was applied. By decreasing the concentration of gelatin to 0.5%, we found that we could introduce gelatin into the material while still maintaining the porous fibrous matrix.

3.4.2 Scaffold morphology

The evaluation of the morphology of the three separate cuff materials uncovered several differences caused by the gelatin incorporation methods. Based on SEM and fiber diameter analysis, it can be seen that gelatin co-spinning leads to a decrease in the average fiber diameter. This is consistent with previous findings that reported that increasing the ratio of gelatin to PCL decreases the average fiber diameter[56]. In our samples, the gelatin content was increased from 0 to 15%, leading to decrease in fiber diameter from 0.536 ± 0.365 µm to 0.267 ± .173 µm. Gelatin coating increased fiber diameter compared to uncoated PCL to .670µm ± .451, as gelatin is added onto the PCL fibers.

As discussed in Chapter 2, increased pore size and porosity is directly correlated to increased fiber diameter[51]. This was consistent with our results for porosity (Figure 10); PCL:gelatin cospun samples had significantly lower porosity than pure PCL samples, and smaller

fiber diameters. Although the gelatin-coated samples had the largest fiber diameters on average, this led to a decrease in porosity compared to pure PCL samples. This apparent increase in fiber diameter is a result of the thickness of the coating on fibers. These trends were also seen in our theoretical pore size measurements with pure PCL samples having the largest average pore diameter, followed by gelatin-coated PCL, and PCL:gelatin cospun samples.

Liquid intrusion is only one method for evaluating porosity, other common methods are gravimetrically, by measuring dimensions of scaffolds and comparing it to weight, and Mercury intrusion porosimetry[63]. The liquid intrusion method is limited by variability introduced by manipulating and blotting samples by hand, and may potentially overestimate porosity due to swelling of fibers by the ethanol. However, Pham et al made a direct comparison of porosity measured in electrospun PCL materials measured by liquid intrusion to porosity measured by gravimetry and mercury porosimetry and found no statistically significant differences between the three methods[63]. Specifics on how blotting and weighing steps are performed are often unreported when using this method for electrospun samples [52,63-65], but it may be possible to decrease variability in the liquid intrusion method by standardizing sample weights and blotting methods. Therefore the porosity data acquired here was done to the best of our ability in accordance with other published work, and will likely be similar to porosity measured through other means.

As discussed previously, pore size and porosity are important to cellular infiltration into materials. All three experimental cuff materials had measured porosities within our target range of 75% to 90%, indicating that all of the candidate cuff materials will likely support smooth muscle cell infiltration[2]. However none of the materials have pore sizes above our designated minimum target of 10μm diameters, which could hamper cellular infiltration. If it is determined that the amount of infiltration into these materials is not adequate for strong tissue cuff integration, other methods for increasing the pore size can be explored; previous studies have suggested using micro-scale fibers, co-spinning with sacrificial fibers and salt leaching to introduce larger pores into the materials[30,50,66].

Gelatin content in the scaffolds was seen through Coomassie Brilliant Blue staining to be fairly evenly distributed in PCL:gelatin cospun samples, but not as much so in gelatin-coated PCL

samples, where the staining appeared less robust. This may indicate that cospinning is a more uniform method for introducing gelatin into PCL materials.

Though not measured directly, it was observed subjectively that the wettability of gelatin incorporated materials, especially PCL:gelatin cospun materials, was greater than pure PCL materials. This is one of the intended impacts of using gelatin blending, as discussed in Chapter 2, however it may impact the performance of assays that involve liquids. It may be possible that when submerged in ethanol during porosity analysis or Coomassie Blue dye that differences in wettability caused differences in interactions between materials and liquids. In order to verify that wettability does not impact these assays, they should be optimized for length of time materials are submerged to ensure that materials are completely wetted without allowing for swelling of fibers.

3.4.3 Mechanical properties

The mechanical testing analysis revealed significant differences in the effects of gelatin incorporation on material properties of cuffs. Co-spinning had the greatest impact on mechanical strength and stiffness of the materials. Co-spinning of gelatin and PCL was found to significantly decrease the ultimate tensile strength of the cuffs compared to both pure PCL cuffs and gelatin-coated cuffs. This is consistent with other findings that gelatin co spinning decreases the overall strength of electrospun constructs[67,68]. Gelatin coating had no impact on the UTS, indicating that the PCL component has the largest influence on mechanical properties. However, despite the significant decrease in strength caused by gelatin co-spinning, the cospun cuff strength is still much higher than the strength reported for completely cell-derived SMC rings, which range from approximately 0.1 - 0.5 MPa[7]. The failure load of cospun cuffs was also about 15 fold greater than the failure load of SMC rings. In previous studies, it has been shown that SMC rings have a load at failure below 0.2N, whereas no electrospun cuffs failed at forces below 2N[7]. This indicates that cuffs can add at least a tenfold increase in strength to the terminal ends of tissue tubes. This increase in strength will improve tube handling during tissue tube fabrication, without risking damage to the construct.

Gelatin incorporation had an impact on the stiffness of materials as well, reflected in the values for elastic modulus and strain at failure. The increase in modulus in gelatin incorporation

samples compared to pure PCL materials was consistent for both PCL:gelatin cospun and gelatin-coated PCL samples. This is consistent with other findings that gelatin electrospun fibers, and gelatin:PCL blended fibers have a much higher elastic modulus than pure PCL fibers[61]. Gelatin incorporation also decreased maximum strain by both coating and cospinning, although significantly more so for cospun samples. Cospun samples may have had a decrease in extensibility since they had a much lower failure load than pure PCL samples. The stiffness of these materials was in a similar range as the stiffness found for SMC rings, which have previously been shown to have elastic moduli ranging from 0.5-2 MPa[7]. The similarities in stiffness between the materials and RASMC tissue is a positive indicator of matching stiffness across a cell derived tissue-cuff construct. This could indicate similarities in compliance between materials and tissue, although compliance cannot be directly measured through ring tensile testing. Compliance can be measured by pressurizing tissues (or electrospun materials) at physiologic ranges and is calculated as change in pressure over change in distension[54]. As discussed in Chapter 2, compliance matching between graft material and tissue is a key feature to developing a patent tissue engineered blood vessel. In future studies, the stiffness match between cuffs and tissue seen here should be further investigated by determining the compliance of cell derived tissue and electrospun cuffs.

3.4.4 Impact of material properties on cuff integration

Overall, mechanical testing revealed that although gelatin incorporation has significant impact on mechanical properties, pure PCL, gelatin-coated PCL, and PCL:gelatin cospun materials have adequate strength to be used as cuffs and add strength to terminal ends of cell derived tubes. The elastic modulus values indicate that there are minimal differences in stiffness between tissue and cuffs. Therefore, PCL and gelatin composite materials fabricated through either coating or cospinning can be potentially used as cuffs for tissue engineered blood vessels. However, cuff integration is as critical to cuff functionality as mechanical strength. The morphology measurements of fiber diameter, porosity, and pore size revealed significant differences that could impact the integration of cuffs and tissue. Based solely on pore size and porosity, it would be expected that the highest degree of infiltration would occur in pure PCL materials, followed by gelatin-coated materials and lastly PCL:gelatin cospun

materials. However, this does not take into account any improvement in SMC attachment and growth caused by gelatin incorporation in cospun PCL:gelatin and gelatin-coated fibers.

Chapter 4. Cellular attachment and outgrowth on cuff materials

4.1 Introduction

The goal of this aim is to determine differences in smooth muscle cell attachment and outgrowth on cuff materials, in order to evaluate the impact of incorporating gelatin into the materials and determine the differences between coating and co-spinning with gelatin. Using attachment and outgrowth assays, these two cellular processes were quantified. The assays used in these studies involve cells seeded directly onto a thin film of electrospun material. These flat sheet models can be used to predict cellular responses in the more complex environment of a cuff in contact with a cell-derived tissue during *in vitro* culture to promote ring fusion.

4.2 Methods

4.2.1 RASMC culture

WKY 3M-22, a rat aortic smooth muscle cell (RASMC) line isolated from 3-month-old adult male Wistar-Kyoto rat aortas[69] were cultured in DMEM (VWR, 45000-324) supplemented with 1% penicillin/streptomycin 100x (VWR, 45000-652) 1,000 I.U. penicillin per mL and 1 mg/mL streptomycin, 1% nonessential amino acid solution (100X stock; VWR 16777-186), 1mM sodium pyruvate (VWR 45000-710) and 2mM L-glutamine (VWR 45001-086). Cells were cultured at 37°C and at 5% CO_2.

4.2.2 Cellular attachment assay

Electrospun samples of each material were placed into the wells of a 12 well plate and held in place using PDMS washers of the same outer dimensions as the well, as seen in Figure 14. Tissue culture plastic wells with PDMS washers were included as control wells. Plates were sterilized via ethelyne oxide sterilization and allowed to degas at least 24 hours before use.

RASMC were trypsinized using 0.25% trypsin for 3-5 minutes and pelleted at 300g for 5 minutes. Cells were then re-suspended to 1X 10^5 cells/mL and 0.5mL of cell suspension was placed into each well (50,000 cells/well). At this time, a standard curve was also seeded in volumes of 450µl of cell suspension per well, with duplicates of 67.5X 10^3 cells/well, 45 X 10^3 cells/well, 30 X 10^3cells/well, 15 X 10^3 cells/well, 7.5 X 10^3cells/well and 0 cells/well. These cells were allowed to attach for 4 hours after which time the supernatant was removed from sample wells and rinsed with 0.5mL of phosphate-buffered saline twice. To measure any background reduction of AlamarBlue® by electrospun materials, 2 samples of each material were prepared as described above but were not seeded with RASMCs. To all sample wells, 0.5mL complete media with 10% AlamarBlue® (Life Technologies, DAL1100) was added. To all standard curve wells, 50µl of AlamarBlue® was added to the 450µl of cell suspension for a final concentration 10% AlamarBlue® in complete media. These samples were then incubated under standard culture conditions for a further 4 hours to allow for the reduction of AlamarBlue® to the fluorescent form, resorufin, by metabolically active cells.

Figure 14: Attachment assay sample preparation. A 12 well plate filled with electrospun material samples placed into the bottom of wells and held in place with PDMS weighting washers.

To quantify AlamarBlue®, two 100µl samples of reduced supernatant were removed from each well and placed in a 96 well plate. Fluorescence was then read in a Victor3 plate reader (Perkin Elmer) at 595nm for 0.1s. This assay was performed twice on two separate batches of electrospun material. The first experimental trial had 6 replicate sample wells and the second experimental trial had 4 replicate sample wells. Data is reported as mean of both experiments ± SEM, n=2. Groups were compared using a one way ANOVA on mean attachment values for each experiment, n=2.

4.2.3 Outgrowth assay

To measure outgrowth, samples were glued into a non-tissue culture treated 6-well plate using silicone medical adhesive and sterilized via ethylene oxide sterilization. Ibidi migration chambers (Ibidi, 80209) were placed onto the materials and a reference line was drawn beneath the chamber on the bottom of the plate. RASMC were dyed with the live cell fluorescent dye, CellTracker Green (Life Technologies, C2925), following manufacturer's instructions for adherent cells, at 10µM dye concentration. Ibidi chambers were then seeded as per the manufacturer's recommendation. Fluorescently-labeled RASMC were trypsinized and re-suspended to $5X10^5$ cells/ml and 70µl of cell suspension was placed into one well of the Ibidi chamber. An Ibidi chamber seeded with RASMC can be seen in Figure 15. Samples were incubated under standard culture conditions for 24 hours, following which the chamber was removed and the well flooded with 2 ml of complete media. Images were acquired approximately every 12 hours for 36 hours and the speed of migration across the material was calculated based on cellular position with respect to the reference line. 4 samples wells were seeded for each experimental group, however due to wicking of cells into the material outside of the seeding region, one pure PCL material sample and one cospun gelatin:PCL well were not measurable, leaving n=3 for those groups and n=4 for the gelatin coated PCL material group. Groups were compared using a one way ANOVA at the $p<0.05$ level, $n\geq3$ as just described.

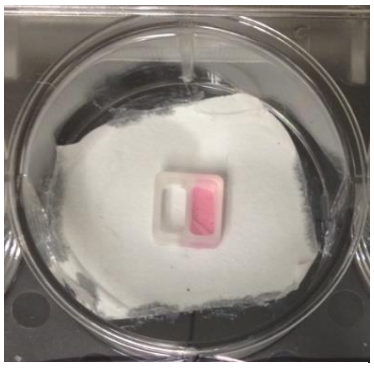

Figure 15: Ibidi chamber seeding. Electrospun PCL:gelatin cospun material, shown glued in place in a 6 well plate and sterilized. Ibidi migration chamber placed onto material and shown seeded with cell suspension. After 24 hours Ibidi chamber was removed and well was flooded with media.

4.3 Results

4.3.1 Attachment of RASMC to cuff materials

4.3.1.1 Assay validation

To validate the AlamarBlue® metabolic assay, a standard curve was developed using known numbers of RASMCs ranging from 0 to 65,000 cells. The linear fit of the standard curve had a coefficient of determination of at least .99. These curves are shown in Appendix A. To determine if there was any reduction of the AlamarBlue® by experimental materials that would impact the measured values, electrospun samples not seeded with RASMC were evaluated with AlamarBlue® to measure background fluorescence. For all three experimental groups background fluorescence was found to not be statistically significantly different from unseeded tissue culture plastic samples, or from the measured "0" value on the standard curve.

4.3.1.2 Attachment Assay Results

The attachment assay revealed differences in the amount of cellular attachment between all different materials; data are shown in Figure 16. Co-spinning with gelatin appears to increase attachment compared to pure PCL alone; On average, approximately 13.3 X 10^3 ± 2.3 RASMC attached to pure PCL fibers, but over 20 X 10^3 RASMCs attached to co-spun samples. Co-

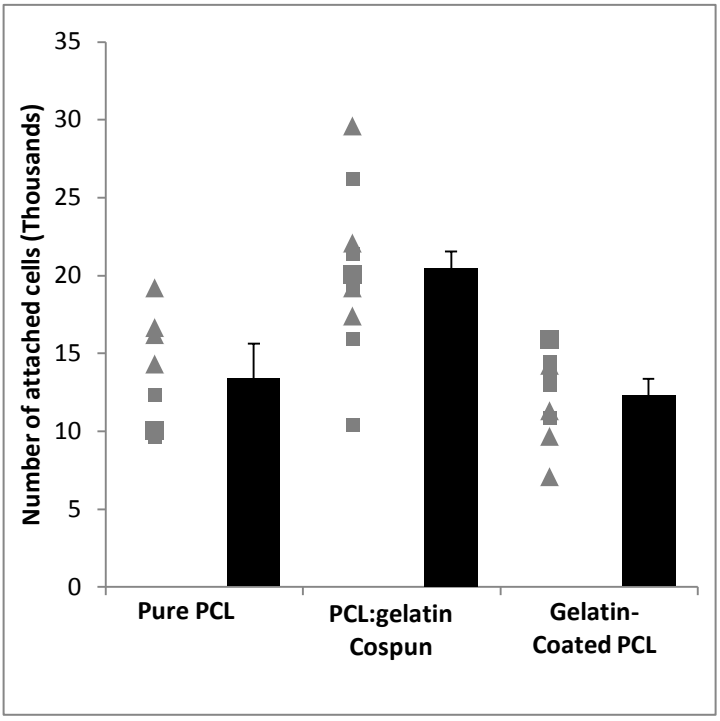

Figure 16: Attachment of RASMC to electrospun materials. AlamarBlue® attachment assay results, reported as number of viable cells detected. Bar displays mean ± SEM for n=2 experiments. ■ indicates individual sample wells from experiment 1 (n=6 sample wells) ▲ indicates individual sample wells from experiment 2 (n=4 sample wells). No statistically significant differences detected, $p>0.05$, for a one way ANOVA between groups (n=2 experiments)

spinning also appears to be more effective than coating for improving attachment, as only 12.2 X 10^3 ± 1.2 attached to gelatin-coated PCL fibers. The tissue culture plastic control was included as a positive control only as due to the two dimensional nature of tissue culture plastic, these samples were not statistically compared to electrospun materials, therefore data were not included in this analysis. However we found that attachment to tissue culture plastic was lower than for electrospun materials.

4.3.2 Outgrowth

Outgrowth of RASMC on cuff materials and tissue culture plastic was evaluated by measuring the width of the region containing fluorescing cells at a reference location at each sample at each time point, and representative samples can be seen in Figure 17. The outgrowth of RASMC over time can be seen in Figure 18. The tissue culture plastic samples had a much faster outgrowth rate from the original seeding zone than all electrospun samples. As with the attachment assay, due to the significant differences in structure between the two dimensional surface of tissue culture plastic compared to the three dimensional structure of an electrospun material, tissue culture plastic control wells were used only as validation that RASMC outgrowth is detectable using this method. RASMCS on all electrospun materials was far lower than on tissue culture plastic and ranged from approximately 140µm to 240µm, compared to the tissue culture plastic outgrowth of 453µm ± 103µm. Although there was positive outgrowth observed over time for all samples, between the three experimental materials, there was not a statistically significant difference in RASMC interaction with materials between the groups. By looking at the total outgrowth distance over 36 hours, summarized in Figure 19, it appears there are minimal differences between groups however outgrowth appears slightly lower on PCL:gelatin cospun materials.

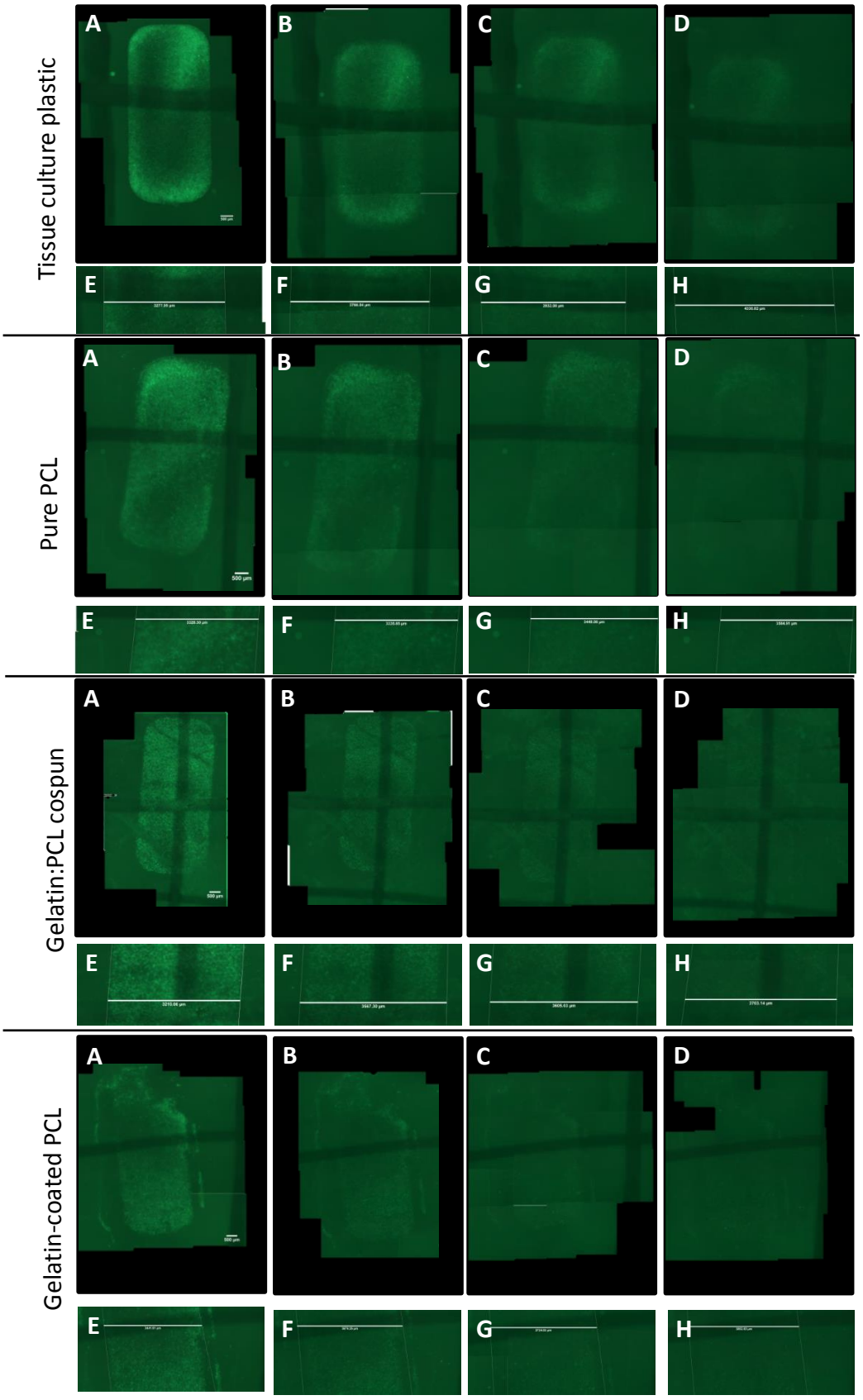

Figure 17: Outgrowth representative images. For each set of images: RASMC at seeding time 0 (A and E), 13 hours (B and F), 23 hours (C and G) and 37 hours (D and H). Top row is stitched 4X images of entire seeding region, bottom row shows cropped image where measurement of outgrowth was made. Each set of images is for a sample of the material listed on left. Scale bar for stitched images shown in panel A is 500µm.

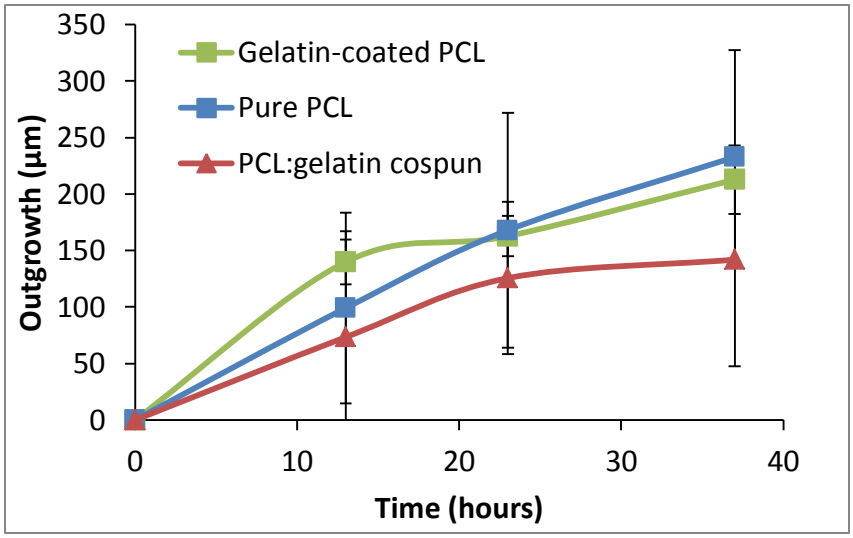

Figure 18: RASMC outgrowth over 36 hours. RASMC outgrowth in µm vs time for all three electrospun material groups reported as mean ± SD. n≥3 for all groups.

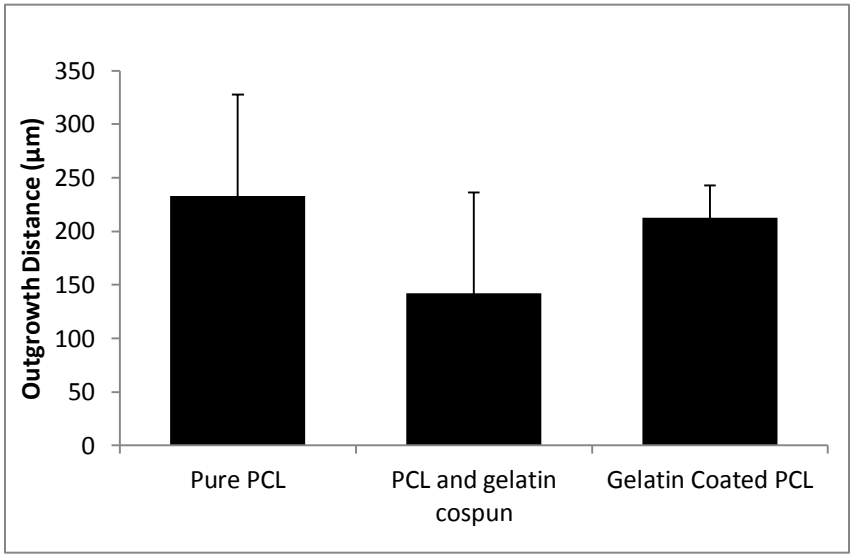

Figure 19: Maximum RASMC outgrowth. Maximum RASMC outgrowth from seeding region after 36 hours for all three electrospun material groups reported as mean ± SD. No statistically significant differences detected between groups for $p<0.05$ (one way ANOVA with Tukey comparisons, n ≥3 individual sample wells in one experiment for all groups.)

4.4 Discussion

The results of these cell attachment and outgrowth evaluation methods showed that gelatin incorporation has a significant impact on cellular adhesion to the electrospun materials, but not on outgrowth. This is consistent with the enhanced cellular adhesion properties of gelatin compared to PCL discussed in Chapter 2, and indicates that gelatin incorporation is capable of imparting these properties to electrospun PCL scaffolds. It appears that gelatin cospinning is more effective at improving RASMC attachment than gelatin coating, based on the higher rate of RASMC attachment on cospun samples than on pure PCL samples. Therefore, we predict that PCL:gelatin cospun materials will lead to the stronger fusion between RASMC tissue derived rings and cuffs, compared to either gelatin-coated or pure PCL fibers, due to greater RASMC adherence to the material.

These overall attachment results give an indication of bulk cellular attachment, not the strength of cellular adhesion, which may also be significantly different between materials. Differences in adhesion strength may also explain the lower attachment of RASMC to tissue culture plastic than to other materials. If PBS washes applied significant shear force, attached cells may have been removed. Blackstone et al have shown that adhesion strength to remove cells from electrospun materials via shear flow is dependent on cell type[70]. Perhaps using a similar method, differences in cellular adhesion strength to materials can be quantified and compared to the rate of bulk attachment determined here. Another possible explanation for the lowered attachment on tissue culture plastic may be the difference in available surface area on an electrospun material compared to a 2D surface, since electrospinning creates a material with very high available surface area. Therefore, it may be possible that 50,000 cells is too high of a seeding density for the 2D surface area available in tissue culture plastic samples, but the higher available surface area in electrospun materials allows for a larger seeding density to be used. It may be necessary to perform more optimization of the seeding densities, washes, and cell numbers to better interpret these findings.

The outgrowth assay did not reveal significant differences between electrospun materials, though RASMC outgrowth was seen to be significantly faster on tissue culture plastic. This may be due to the three dimensional nature of an electrospun material allowing outgrowth in more than x and y directions. It was also found that outgrowth did not correlate to cellular attachment. This indicates that these two cellular processes, outgrowth and attachment, are not necessarily related. It is also possible, since the overall trends for outgrowth were opposite of the overall trends for attachment, that as cells are better adhered to a material, the outgrowth rate decreases. Outgrowth has been shown to be directly related to fiber alignment in electrospun materials[71]. No particular fiber alignment was created in these materials, which may explain the overall low outgrowth rate.

These assays allow for the quantification of RASMC outgrowth and attachment, and may be able to be used in the future as screens to narrow down a wide range of candidate cuff materials. From the results of these assays, we predict that the cospun PCL:gelatin materials

will integrate better than pure PCL samples or gelatin-coated PCL materials with RASMC tissue rings. Therefore, the next step was to test these hypotheses with 3D tissue cuff fusion.

Chapter 5. Cuff integration with 3D cell derived tissues

5.1 Introduction

The characterization of material morphology, mechanical properties, cellular outgrowth and attachment can provide an indication of how successfully the material will perform as a cuff, but the ultimate test is to examine cuff integration with cell derived ring tubes. The main features of the cuff-tissue integration are the strength of the bond between the cuff and the tissue, the amount of cell growth out on the surface of the cuff and the amount of infiltration into the cuff material. By comparing these properties between the experimental cuff materials, the effect of incorporating gelatin into a PCL scaffold on cuff-tissue integration, the effect of the method of incorporating gelatin (coating or co-spinning) on cuff integration, and the predictive power of electrospun material properties (e.g. cell attachment, material morphology, cellular outgrowth) can be determined.

5.2 Methods

5.2.1 Ring formation

Self-assembled rings were formed as described by Gwyther et al[7]. Briefly, 2% agarose in DMEM was melted via autoclaving and poured into custom PDMS molds containing 5 annular wells with 2mm diameter posts. After the agarose cools, the mold is placed in a 6 well plate and equilibrated in 1.5 mL of complete media for at least 12 hours prior to seeding. RASMCs were cultured as described in Chapter 4. Cells were trypsinized and re-suspended to 10 $X10^6$ cells/mL and 50µl of cell suspension (500,000 cells) was seeded into each ring-shaped agarose well. Cells were allowed to aggregate and contract around the central post overnight and wells were flooded with complete media to submerge the agarose wells. Rings were cultured for an additional 2 days prior to tube fusion.

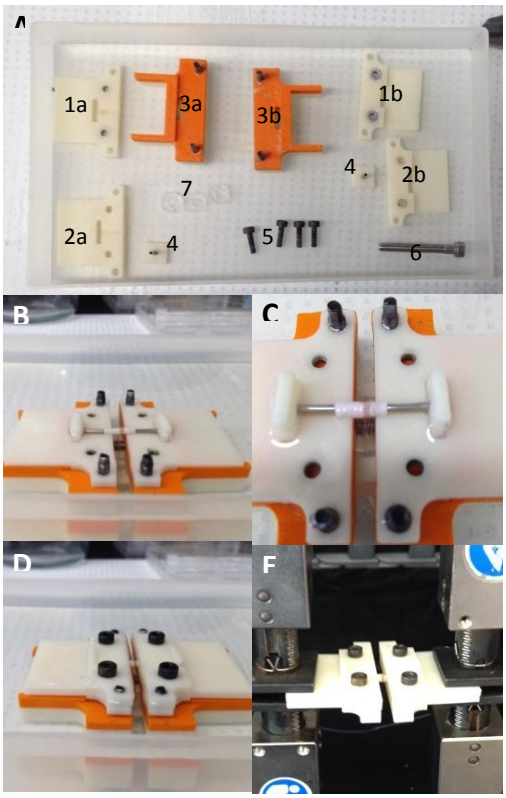

Figure 20: Custom grip loading. A) All grip pieces. 1-Grip bottom pieces (a-face up, b-face down), 2- Grip top pieces (a-face up, b face down), 3-base jig pieces, 4-cannulating posts, 5-M3 screws for grips, 6-#10 screw for base jigs, 7-PDMS spacers. **B)** Base jig loaded with spacers. **C)** Tube with PCL cuffs loaded onto bottom pieces and cannulating posts. **D)** Top grip pieces clamped in place. **E)** Grips and tube loaded into Instron ElectroPuls screw action grips.

5.2.2 Tube fusion

Cuff materials were fabricated as described in Chapter 3. Cuffs were sterilized using ethylene oxide and allowed to de-gas in the sterilization pouches for 24 hours before use. Tubes were formed as described by Gwyther et al [7]. Briefly, 3-day-old rings were removed from agarose molds and stacked on silicone tubing of 2mm outer diameter. Sterilized cuffs were also stacked on either end of each ring tube. For longitudinal pull to failure testing, tubes were made of 2 cuffs and 5 RASMC rings. These tubes were placed in a custom polycarbonate holder to suspend tubes in complete media. Tubes were cultured for 7 days prior to mechanical testing and fixing.

5.2.3 Longitudinal pull to failure

5.2.3.1 Custom Grips

In order to maintain the tubular shape of constructs, custom grips were designed and fabricated that cannulate and clamp tubular tissue constructs similar to grips described by Carolyn Rae Berry for testing vascular prostheses[72]. According to the drawings in Appendix B, the grips, cannulation post bases, and base jigs were printed on a Dimension SST 1200es 3D printer. Two M3 hex nuts were placed into both bottom grip pieces, a #10 hex nut was placed into the base jig piece, and two M3 socket cap screws were placed into both base jig pieces. Two 14G blunt-ended syringe tips were removed from plastic caps and inserted and glued into cannulation post bases to form cannulation posts. All pieces were sanded until they easily fit together. PDMS washers of approximately 3-4mm thickness were used as spacers. Images of the tissue tube loading process are shown in Figure 20.

5.2.3.2 Testing protocol

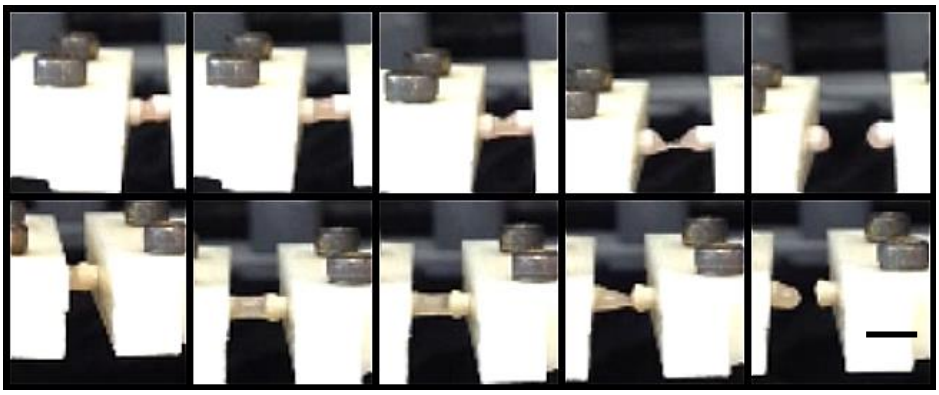

Figure 21: Sample modes of failure. Example failure locations shown for tubes with cuffs. Top row shows failure of tube with gelatin and PCL cospun cuffs “in tissue”, and bottom row shows failure of tube with gelatin coated PCL cuffs “at interface”. From right to left images show tubes at loading, fully extended, just prior to failure, at failure, and after failure. Scale bar is 3mm.

Tubes in custom grips were loaded into Instron ElectroPuls E1000 screw action clamp grips with a 50N load cell. Using Instron Blue Hill software, tubes were pulled to failure at 50mm/min in accordance with ISO 7198:1998 standards for testing vascular prostheses[58]. The failure location was noted as either “at cuff tissue interface”, “in tissue”, or “in cuff material”. Figure 21 shows representative images of “in tissue”, and “at interface” failures, no “in cuff material” failures were observed. Using a MatLab script, the maximum load was calculated for each tube.

5.2.4 Histology

Following mechanical testing, tubes were fixed in 10% Neutral Buffered Formalin for 1 hour and stored in 30% sucrose prior to embedding. Samples were embedded in OCT compound and frozen at -20°C . Samples were sectioned on a cryostat, and stained with Hoechst 33342 to visualize nuclei.

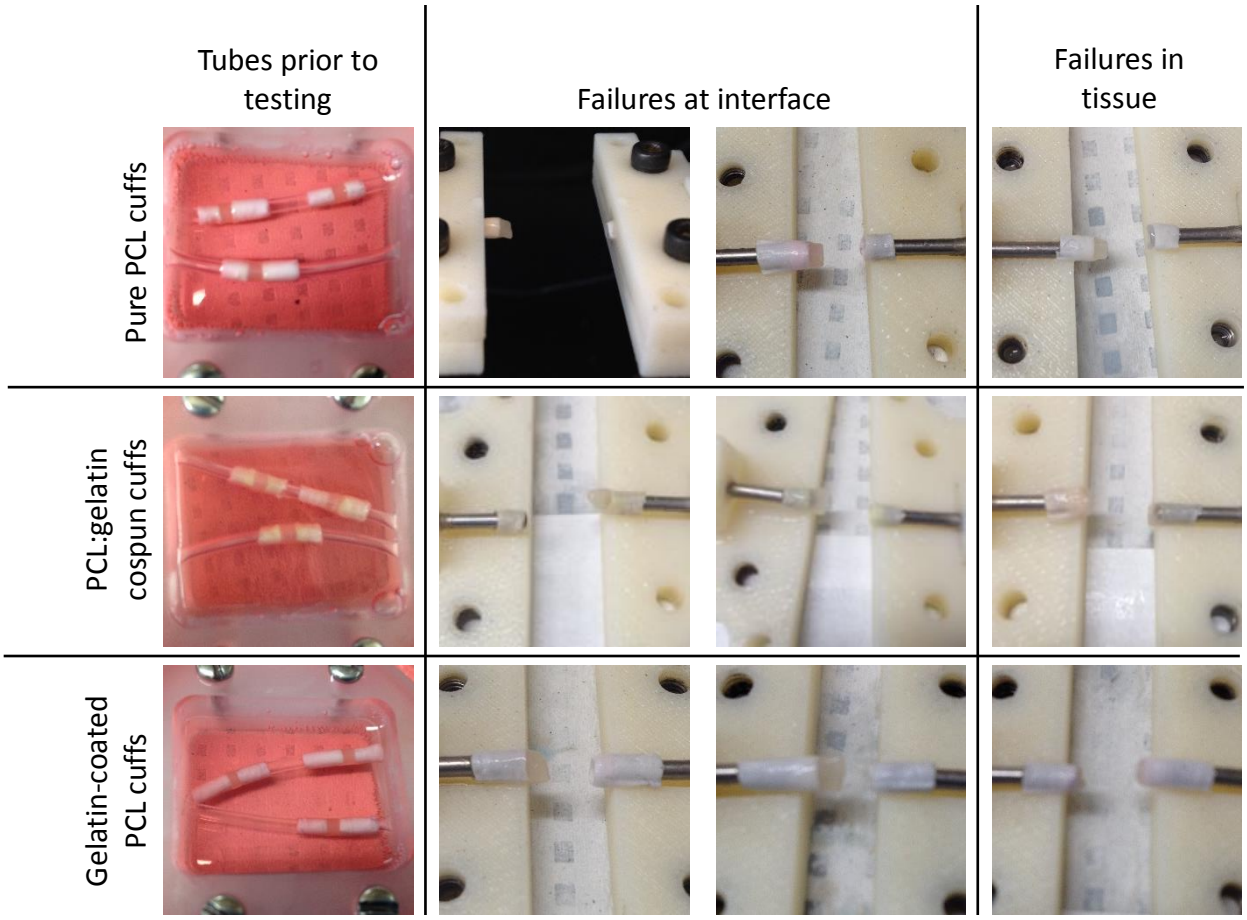

Figure 22: RASMC ring/cuff tubes post longitudinal pull to failure. Tubes before and after longitudinal pull to failure testing displaying failure location.

5.3 Results

5.3.1 Longitudinal pull to failure

Longitudinal pull to failure testing was used to reveal differences in strength of tissue cuff interfaces between the three experimental cuff materials. For all tubes, the failure location was categorized as either within tissue or at tissue cuff interface. There was no discernable difference in failure location for all tube types. For all experimental groups, two tubes failed at the tissue/cuff interface and one tube failed in the tissue. Tubes post failure can be seen in Figure 22. Load extension data was recorded for all tubes and the maximum load was calculated. However, all tubes failed below 100mN, which is below the measurement threshold of the load cell; therefore load at failure could not be accurately determined. There was a large degree of variability in maximum load, but there appears to be a trend towards PCL:gelatin

cospun tubes having the highest longitudinal strength, followed by gelatin-coated PCL samples and pure PCL cuffs were the weakest constructs. Maximum load data can be seen in Figure 23.

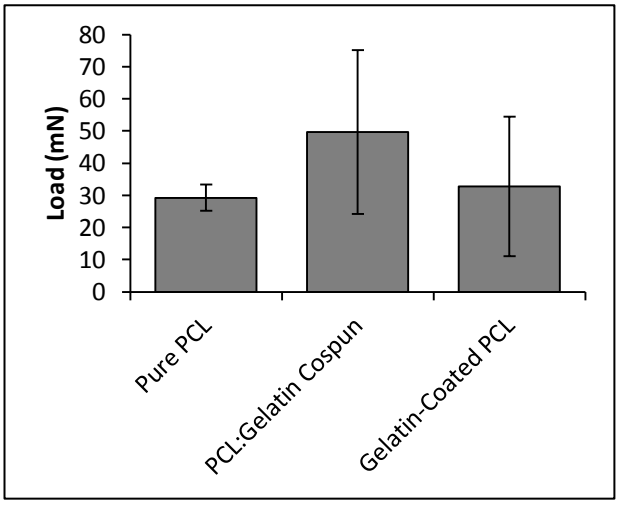

Figure 23: Maximum longitudinal load. Maximum load recorded during longitudinal testing, of constructs containing 2 cuffs of material and 5 RASMC rings. No statistical significance detected between groups using a one-way ANOVA. n=3 for all groups.

5.3.2 Histology

Tissue tubes from pull to failure testing were fixed and sectioned to visualize RASMC outgrowth and integration with cuffs. Nuclear staining was used to visualize the number and location of RASMC on cuffs. All tubes integrated with experimental cuff composites via RASMC outgrowth over the outer and inner surface of the cuffs and RASMC infiltration into cuffs as can be seen in Figure 25. There appears to be a similar amount of RASMC infiltration into pure PCL and gelatin-coated cuffs. In contrast, PCL:gelatin cospun cuffs appeared to have RASMC infiltration throughout the thickness of the cuffs. However, although all samples were spun using the same parameters, cospun cuffs appear to be thinner overall. The thickness of the layer of tissue outgrowth varied between cuff types. Pure PCL cuffs appear to have a tissue layer approximately 30 microns thick on the outside surface and a thin tissue layer on inner surface Gelatin-coated cuffs appear to have a tissue layer of approximately equal thickness on both cuff surfaces. There also appears to be a much thicker layer of RASMC on the surface of gelatin:PCL cospun cuffs compared to the other two groups, on both the outer and inner surfaces.

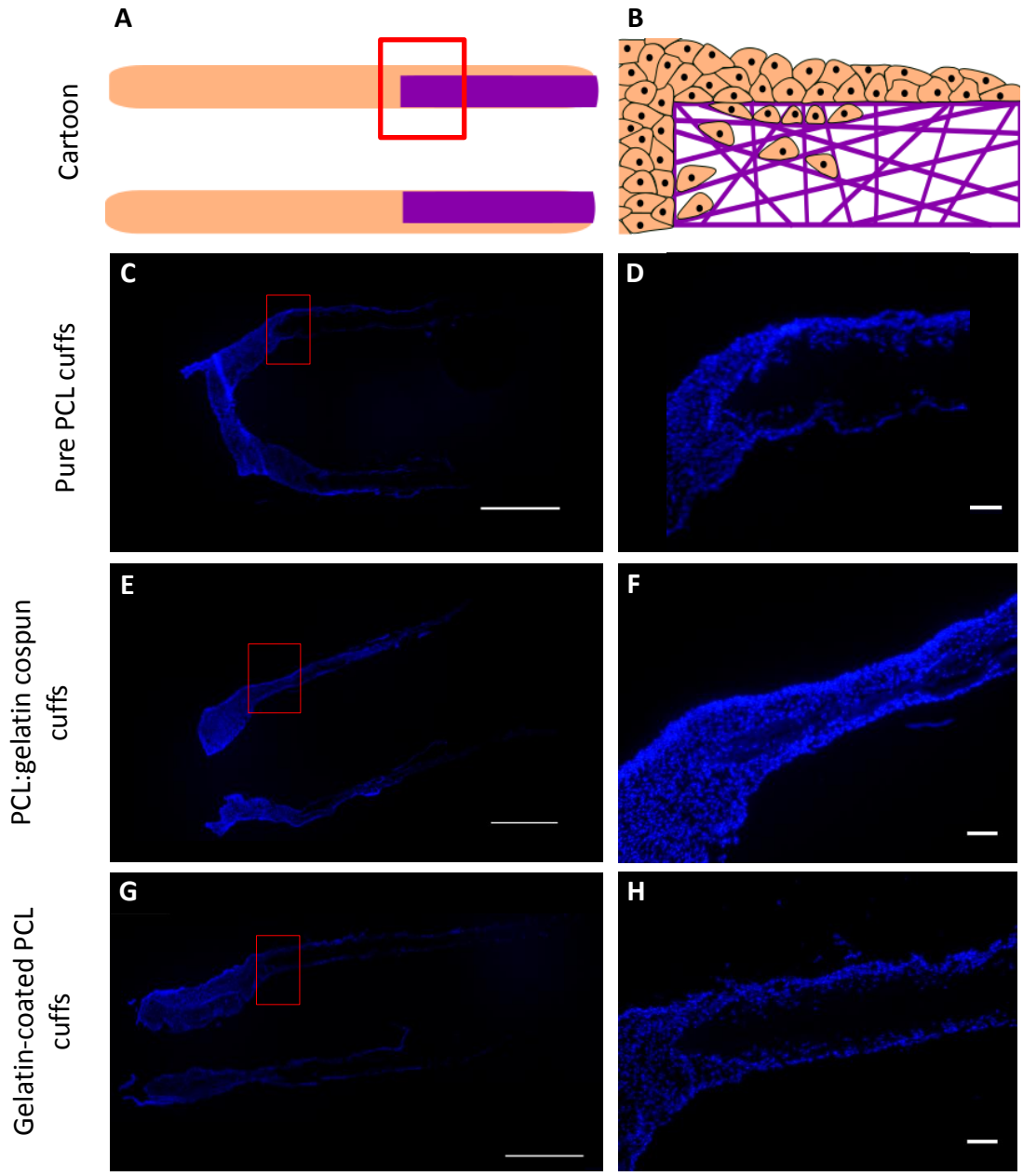

Figure 25: Hoechst staining of tissue cuff constructs following mechanical testing. **A,** Cartoon showing orientation of sections of tubes for images in the left column and **B,** the right column. Representative 4X merged images of tubes with **C,** pure PCL cuffs, **E,** PCL:gelatin cospun cuffs and **G**, gelatin-coated PCL cuffs. Tissue is oriented to the left and cuffs are oriented to the right, red box indicates region displayed in right column panels. **D,F,H)** 10X images of tissue cuff interface, again tissue is oriented to the left, and cuff material is oriented to the right. Lumen of tube is the bottom of the image, scale bar is 100µm. Images have had brightness and contrast enhanced equally across images to improve visibility of blue fluorescent nuclei.

5.4 Discussion

5.4.1 Mechanical testing

Although mechanical testing did not reveal significant differences in maximum load, the overall method of tube cuff failure indicates that tubes and cuffs have been well integrated. For all experimental cuff materials, no failures occurred within the cuff material, and cuffs did not appear significantly damaged by testing as can be seen in post failure tubes in Figure 22. This was expected based on the UTS and failure load of cuffs measured in chapter 3, as these values were well above any load measured in this test. For all materials, one tube out of three failed within the tissue instead of at the interface, this could indicate that any manipulation performed on the tube, particularly longitudinally, which would cause failure of the cuff tissue bond, also has a high likelihood of causing failure of the tissue itself. However due to the failure loads below 50mN, which is below the resolution of this test protocol, it is difficult to make any distinctions between the different materials. In order to make conclusions about tissue or bond strength, maximum loads at interface and tissue failure need to be quantified.

5.4.2 Histological evaluation

Histological evaluation revealed the extent of tissue cuff integration via RASMC outgrowth and infiltration into cuffs. These findings indicate that gelatin incorporation method significantly impacts the extent of cuff integration. The thicker tissue outgrowth over the surface of the cuff indicates higher affinity of RASMC to cospun cuff materials compared to pure PCL materials, or gelatin coated materials. Infiltration also appears to be most prevalent in cospun samples and occurs throughout the entire length of the cuffs throughout the entire cuff thickness. Therefore gelatin cospinning can be successfully used to improve tissue cuff integration, and was found to me more effective than gelatin coating. Going forward, gelatin cospinning should be used to fabricate cuffs for cell derived ring TEBV.

Chapter 6. Conclusions and future work

6.1 Conclusions

6.1.1 Cuffs as tools for developing tissue engineered blood vessels

The overall findings of this work indicate that PCL and gelatin incorporated PCL cuffs can be successfully used for the designed purpose: to increase strength of TEBV terminal ends and extend the length to make completely cell derived constructs easier to handle through cellular attachment and growth on cuff materials. We have also shown that gelatin incorporation has a distinct impact on the properties of electrospun PCL materials and that the method chosen to accomplish this incorporation can have widely varied effects. In particular, these studies have indicated that gelatin cospinning is a strong candidate for improving cellular attachment and cuff integration with tissues, and that although gelatin coating may maintain mechanical strength of materials, it may not be as effective at improving attachment and cuff integration. Compared to other previously used cuff materials our approach here focused on designing for cellular interactions with the material as opposed to exclusively mechanical properties. The Tranquillo group's PLA cuffs were designed specifically to add suture retention strength and the Niklason Dacron arms were designed to attach tubes to a bioreactor, but neither examined how the growth of cells in constructs could improve cuff and tissue integration[17,18]. By using the PCL and gelatin cospun cuffs described here, cuff tissue fusion may be improved and could lead to better cuff incorporation in these other cell based systems that depend on strong tissue material integration.

6.1.2 Cospinning is an effective method for gelatin incorporation within electrospun PCL materials

The direct comparison of the impact of gelatin incorporation methods on electrospun materials has been explored by other groups but previous work has not provided a direct comparison of coating and cospinning before[56]. Chen et al compared three other methods for creating blended PCL and gelatin fibers, and the impact on material properties, however coating with gelatin was not included in the compared methods, nor were cellular

interactions[56]. Here, we were able to determine the impact of gelatin incorporation on material properties as well as on cellular interaction. By designing a material with both of these features in mind, a more comprehensive choice can be made on what is the most appropriate material for our application.

From our results, it appears that the method of gelatin incorporation can directly impact the performance of the scaffold material, and that for maximum cellular integration from cell derived tissues, cospinning is more effective than gelatin coating. Cospinning is also a more expedient and cost effective process compared to coating. Coating requires an extra post-processing step that requires additional equipment and reagents and adds significant time to fabrication. This increase in complexity, time, and cost is summarized in Table 5, and shows that using this coating process increases cost 3 fold over cospinning and nearly triples fabrication time. It was seen, however, that cospinning decreases overall strength of the materials, but for the purposes of developing cuffs for cell-derived TEBV, the strength of cospun materials is still greater than the tissue. The added benefit of improved strength of gelatin-coated PCL does not therefore outweigh the benefits of improved cellular attachment and integration of gelatin and PCL cospun samples.

Table 5: Resources, cost and time required for fabricating gelatin incorporated cuffs by coating or cospinning. Materials, cost, and time needed to spin one mandrel of cuffs (cost of each reagent rounded to nearest dollar)

	Gelatin coating of PCL fibers	Gelatin cospinning with PCL
Materials needed	120mg of PCL 50mg of gelatin 1 mL of TFE 2mg of genipin Saturated glycine 0.1M NaH_2PO_4	102mg of PCL 18mg of gelatin 1mL of TFE 3µl of Acetic acid
Approximate cost	$13	$4
Time required	12 hours to dissolve PCL in TFE 12 minutes to electrospin 8.5 hours for gelatin coating process 12 hours to air dry materials **Total: approximately 33 hours**	12 hours to dissolve Gelatin and PCL in TFE 12 minutes to electrospin **Total: approximately 12 hours**

6.1.3 Predicting material integration with 3D cell derived tissues

One major goal of evaluating morphology of cuff materials and SMC attachment and outgrowth was to determine which parameters are most predictive of successful tissue cuff integration. Histological evaluation of cuff tissue interfaces showed trends that agreed with results predicted by the attachment assay. Cospun cuffs were found to support cellular outgrowth and integration in 3D more readily than either pure PCL or gelatin-coated PCL cuffs, consistent with findings for SMC attachment to these materials. This could indicate that the attachment assay is a good predictor of cuff performance, over outgrowth or scaffold morphology. As noted in Chapter 3, based solely on morphology information, pure PCL samples were predicted to have the greatest amount of SMC infiltration, as they had porosity and pore sizes closer to our defined targets than PCL:gelatin cospun samples. However, based on the histological results, the cuff structure was not as influential as the cellular adhesive properties of the materials as measured by the attachment assay. Though cuff integration of Pure PCL cuffs may have been improved by having the desired scaffold morphology, if materials are to be screened for fusion with cell derived tissues, attachment appears most likely to predict success.

6.2 Future work

Overall in the future, we would like to explore how the material properties of cuffs impact cellular interactions and ultimately cuff integration. By looking more closely at the wettability, gelatin content and fiber alignment, we may be able to gain more meaningful insight into the results from our cellular interaction data. This knowledge can then be applied to any future modifications made to cuff materials to improve outgrowth attachment or infiltration. Once these final modifications have been made, these cuffs can be used in future iterations of our TEBV fabrication system, such as the application of cuffs to human TEBV and tissue tubes made using other cells types.

6.2.1 Further analyze differences in material properties between experimental cuff materials

6.2.1.1 Determine the effect of fiber alignment in electrospun materials

One feature of the cuff materials that has not been quantified is the alignment of fibers. Alignment has been shown to affect cellular phenotype, morphology, and migration[71,73-76]. Here

we did not attempt to modify alignment of fibers though it has been shown that smooth muscle cells orient along aligned fibers and may exhibit a switch to a more contractile phenotype, therefore cuff tissue integration may be also be impacted by fiber alignment[73,77]. Using different collector geometries, such as cones, or modifying the electric field, or the rotational speed of the mandrel, alignment of fibers can be controlled[76,78,79]. Using these methods, cuffs with random and aligned nanofibers can be fabricated and the cellular outgrowth and cuff integration can be compared to determine the impact of alignment. Alignment has also been shown to effect modulus and tensile strength, with both parameters increasing in the direction of alignment, so mechanical analysis of aligned and non-aligned cuffs should also be performed[80].

6.2.1.2 Impact of gelatin content in cuff materials

Here we compared methods for incorporating gelatin, however we did not explore how the amount of protein incorporated impacts cuff materials. We have seen that PCL and gelatin cospun cuffs integrated most completely with tissues, however we did not quantify how the varying the amount of gelatin impacts cellular outgrowth and infiltration or the mechanical properties. It has previously been shown that the ratio of gelatin and PCL in electrospun scaffolds effects the elastic modulus[44]. So in order to determine how gelatin affects cuff suitability it should be determined what ratio of gelatin to PCL leads to the best cuff tissue integration while maintaining the necessary mechanical properties. The amount of gelatin in the materials can also be directly quantified. Here we used a Coomassie Brilliant Blue stain to visualize the gelatin content, but that method can be modified to quantify gelatin content in the form of a modified Bradford assay[81-83]. This would allow for a direct measure of the ratio of gelatin to PCL and allow us to study how this ratio affects tissue cuff integration and mechanical properties.

6.2.2 Analyze the impact of variability in electrospun materials

Electrospinning is known to be affected by environmental parameters such as temperature and humidity, as it is highly dependent on the atmospheric conditions for the generation of the electric field dynamics critical to fiber formation [25]. For each experiment here,

a single batch of each experimental material was fabricated and analyzed. In order to confirm these results, these studies should be repeated with several batches of material to determine whether batch to batch variability impacts the overall conclusions reached here.

The impact of using different collectors on variability should also be determined. For the cellular attachment and outgrowth assays performed here, the material was spun onto a flat collector as opposed to a rotating mandrel. By using the characterization methods described here, a comparison could be made between fibers collected on each surface and verify that there are no major differences between the materials, and that cellular interactions are similar regardless of collector used.

Lastly, the fiber diameter measurements, porosity calculations, mechanical tests, outgrowth and fusion studies were each performed once, and each on a single batch of electrospun cuff materials, therefore experiment to experiment variability has not been accounted for. By increasing the number of experimental replicates these results can more robustly be used to predict cuff performance.

6.2.3 Improve resolution of testing protocols

6.2.3.1 Increasing time scale outgrowth measurements

This outgrowth assay was successfully used to measure RASMC outgrowth over 36 hours, however due to the limitations of retention of the CellTracker dye, this assay could not be extended any further in time. Due to the nature of CellTracker dye, which stains the cytoplasm of cells, following every cell division a signal from an individual cell decreases by half. Therefore signal fading during outgrowth that occurs due to cell division becomes a nontrivial problem for measuring maximum outgrowth over long periods of time. Jain et al, describe using a similar process to measure outgrowth of intracortical tumor cells on electrospun fibers, over a much longer time period than was studied here, by using GFP transfected cells, thus eliminating the signal fading issue[46]. If GFP transfection is not feasible, it may be possible to dye RASMC with CellTracker prior to each imaging session to refresh the fluorescent signal. RASMC have a relatively short doubling time, less than 24 hour hours in our experience, and if these studies are to be carried out over a longer time period it may be necessary to minimize the effect of

proliferation entirely and only evaluate migration by halting mitosis in RASMC by pretreating cells with a mitotic inhibitor such as mitomycin-C[84].

6.2.3.2 Improving the resolution of longitudinal pull to failure testing

As described in Chapter 5, the longitudinal testing results did not reveal significant differences in failure load experienced by tubes with different cuff materials. In order to improve the resolution of the testing protocol, we recommend decreasing the extension rate applied to tissue, and replacing the high range 50N load cell with a smaller range, more sensitive 1N load cell. By decreasing the extension rate, this testing would no longer meet the qualifications for ISO vascular graft testing described in Chapter 5, as 50mm/min is the lowest recommended strain rate, but at this stage of graft development, modifying the standard protocol may be necessary to acquire more sensitive data. There is precedent for testing vessels at much lower strain rates, down to 1mm/min, which may yield more consistent results[60]. With these modifications a clearer difference may emerge between the different cuff materials in either failure location or load at failure.

6.2.4 Broader applications of electrospun cuffs

Building on the work presented here, electrospun PCL and gelatin cuffs can be used as effective research tools for creating TEBV. One of the most important next steps for cell derived ring fused tubes is to use human primary smooth muscle cells (HSMC) to create vessels that much more closely model human vascular tissue. By completing tube fusion studies using cuffs and HSMC cell derived tubes, the application of this system across cell types can be evaluated. As discussed in Chapter 2, several other tissue engineered blood vessels already employ some type of cuff to reinforce and lengthen tubes, so a direct comparison between the cuff materials used in these systems and cospun PCL:gelatin cuffs could be used to determine the applicability of these cuffs across platforms. The ring system is also not limited to vascular tissue engineering, recently Dikina et al have shown that it can be applied to tracheal tissue engineering, and it would be interesting to see if this tool is effective and beneficial across cell types and applications[85].

Citations

1 Ju, Y. M., Choi, J. S., Atala, A., Yoo, J. J. & Lee, S. J. Bilayered scaffold for engineering cellularized blood vessels. *Biomaterials* **31**, 4313-4321 (2010).

2 Zeltinger, J., Sherwood, J. K., Graham, D. A., Müeller, R. & Griffith, L. G. Effect of pore size and void fraction on cellular adhesion, proliferation, and matrix deposition. *Tissue engineering* **7**, 557-572 (2001).

3 Fu, W. *et al.* Electrospun gelatin/PCL and collagen/PLCL scaffolds for vascular tissue engineering. *International journal of nanomedicine* **9**, 2335 (2014).

4 World Health Organization, Global status report on noncommunicable diseases 2010 (Ringgold Inc, Portland, 2011).

5 Go, A. S. Heart Disease and Stroke Statistics–2014 Update: A Report from the American Heart Association. *Circulation* **18**, 209-209 (2014).

6 Seifu, D. G., Purnama, A., Mequanint, K. & Mantovani, D. Small-diameter vascular tissue engineering. *Nature reviews. Cardiology* **10**, 410 (2013).

7 Gwyther, T. A. *et al.* Engineered vascular tissue fabricated from aggregated smooth muscle cells. *Cells, tissues, organs* **194**, 13-24 (2011).

8 Rabih, O. D. *et al.* Antimicrobial Activity of Prosthetic Heart Valve Sewing Cuffs Coated With Minocycline and Rifampin. *Antimicrobial Agents and Chemotherapy* **46**, 543-545 (2002).

9 Klaco, T. & Carbomedics, Sewing cuff assembly for heart valves. US Patent US6716244 B2 (2004).

10 Tiwari, A., Cheng, K. S., Salacinski, H., Hamilton, G. & Seifalian, A. M. Improving the patency of vascular bypass grafts: The role of suture materials and surgical techniques on reducing anastomotic compliance mismatch. *European Journal of Vascular & Endovascular Surgery* **25**, 287-295 (2003).

11 Ducasse, E. *et al.* Interposition Vein Cuff and Intimal Hyperplasia: An Experimental Study. *European Journal of Vascular and Endovascular Surgery* **27**, 617-621 (2004).

12 Werker, P. M. N. & Kon, M. Review of facilitated approaches to vascular anastomosis surgery. *The Annals of Thoracic Surgery* **63**, S122-S127 (1997).

13 Watanabe, T., Kanda, K., Ishibashi-Ueda, H., Yaku, H. & Nakayama, Y. Development of biotube vascular grafts incorporating cuffs for easy implantation. *Journal of artificial organs* **10**, 10-15 (2007).

14 Yamanami, M. *et al.* Implantation study of small-caliber "biotube" vascular grafts in a rat model. *Journal of artificial organs : the official journal of the Japanese Society for Artificial Organs* **16**, 59-65 (2013).
15 Watanabe, T., Kanda, K., Ishibashi-Ueda, H., Yaku, H. & Nakayama, Y. Autologous small-caliber "biotube" vascular grafts with argatroban loading: a histomorphological examination after implantation to rabbits. *Journal of biomedical materials research. Part B, Applied biomaterials* **92**, 236-242 (2010).
16 Prabhakar, V. *et al.* Engineering porcine arteries: Effects of scaffold modification. *Journal of Biomedical Materials Research Part A* **67A**, 303-311 (2003).
17 Huang, A. H. & Niklason, L. E. Engineering biological-based vascular grafts using a pulsatile bioreactor. *Journal of Visualized Experiments* (2011).
18 Syedain, Z. H., Meier, L. A., Bjork, J. W., Lee, A. & Tranquillo, R. T. Implantable arterial grafts from human fibroblasts and fibrin using a multi-graft pulsed flow-stretch bioreactor with noninvasive strength monitoring. *Biomaterials* **32**, 714-722 (2011).
19 Formhals, A. Process and apparatus for preparing artificial threads. US patent US1975504 A (1934)
20 Pham, Q. P., Sharma, U. & Mikos, A. G. Electrospinning of polymeric nanofibers for tissue engineering applications: a review. *Tissue engineering* **12**, 1197-1211 (2006).
21 Leach, M. K., Feng, Z.-Q., Tuck, S. J. & Corey, J. M. Electrospinning fundamentals: optimizing solution and apparatus parameters. *Journal of Visualized Experiments* (2011).
22 Wendorff, J. H., Agarwal, S. P., Greiner, A. *Electrospinning: materials, processing, and applications*. (Wiley-VCH, 2012).
23 Bhardwaj, N. & Kundu, S. C. Electrospinning: A fascinating fiber fabrication technique. *Biotechnology Advances* **28**, 325-347 (2010).
24 Reneker, D. H. & Chun, I. Nanometre diameter fibres of polymer, produced by electrospinning. *Nanotechnology* **7**, 216 (1996).
25 Fernández de la Mora, J. The Fluid Dynamics of Taylor Cones. *Annual Review of Fluid Mechanics* **39**, 217-243 (2007).
26 Shin, Y. M., Hohman, M. M., Brenner, M. P. & Rutledge, G. C. Electrospinning: A whipping fluid jet generates submicron polymer fibers. *Applied Physics Letters* **78**, 1149-1151 (2001).
27 Chang, W. N. *Nanofibers: Fabrication, Performance, and Applications*. (Nova Science Publishers, Inc, 2009).

28 Hasan, A. *et al.* Electrospun scaffolds for tissue engineering of vascular grafts. *Acta biomaterialia* **10**, 11-25 (2014).
29 Moreno, M. J. *et al.* Development of a compliant and cytocompatible micro-fibrous polyethylene terephthalate vascular scaffold. *Journal of Biomedical Materials Research Part B: Applied Biomaterials* **97B**, 201-214 (2011).
30 Marion, v. M. H. *et al.* Tailoring fiber diameter in electrospun PCL scaffolds for optimal cellular infiltration in cardiovascular tissue engineering. *Tissue engineering. Part A* **15** (2009).
31 Pfeiffer, D. *et al.* Endothelialization of electrospun polycaprolactone (PCL) small caliber vascular grafts spun from different polymer blends. *Journal of Biomedical Materials Research Part A* **102**, 4500-4509 (2014).
32 Ma, Z., He, W., Yong, T. & Ramakrishna, S. Grafting of gelatin on electrospun poly(caprolactone) nanofibers to improve endothelial cell spreading and proliferation and to control cell orientation. *Tissue engineering* **11**, 1149-1158 (2005).
33 Rocco, K. A., Maxfield, M. W., Best, C. A., Dean, E. W. & Breuer, C. K. In vivo applications of electrospun tissue-engineered vascular grafts: a review. *Tissue engineering. Part B* **20**, 628 (2014).
34 Bergmeister, H. *et al.* Electrospun small-diameter polyurethane vascular grafts: ingrowth and differentiation of vascular-specific host cells. *Artificial organs* **36**, 54-61 (2012).
35 Grasl, C., Bergmeister, H., Stoiber, M., Schima, H. & Weigel, G. Electrospun polyurethane vascular grafts: in vitro mechanical behavior and endothelial adhesion molecule expression. *Journal of biomedical materials research. Part A* **93**, 716 (2010).
36 Jia, L., Prabhakaran, M. P., Qin, X., Kai, D. & Ramakrishna, S. Biocompatibility evaluation of protein-incorporated electrospun polyurethane-based scaffolds with smooth muscle cells for vascular tissue engineering. *Journal of Materials Science* **48**, 5113-5124 (2013).
37 Khorasani, M. T. & Shorgashti, S. Fabrication of microporous polyurethane by spray phase inversion method as small diameter vascular grafts material. *Journal of Biomedical Materials Research Part A* **77A**, 253-260 (2006).
38 Cipitria, A., Skelton, A., Dargaville, T. R., Dalton, P. D. & Hutmacher, D. W. Design, fabrication and characterization of PCL electrospun scaffolds—a review. *Journal of Materials Chemistry* **21**, 9419 (2011).

39 Ayres, C. E., Bowlin, G. L. & Simpson, D. G. 012 Microvascular Endothelial Cell Migration in Scaffolds of Electrospun Collagen. *Wound Repair and Regeneration* **13**, A4-A27 (2005).
40 Boland, E. D. *et al.* Electrospinning collagen and elastin: preliminary vascular tissue engineering. *Frontiers in bioscience : a journal and virtual library* **9**, 1422 (2004).
41 Lee, S. J. *et al.* Development of a composite vascular scaffolding system that withstands physiological vascular conditions. *Biomaterials* **29**, 2891-2898 (2008).
42 Heydarkhan-Hagvall, S. *et al.* Three-dimensional electrospun ECM-based hybrid scaffolds for cardiovascular tissue engineering. *Biomaterials* **29**, 2907-2914 (2008).
43 Yamamoto, M., Yamamoto, K., Yamato, M. & Aoyagi, M. Identification of Integrins Involved in Cell Adhesion to Native and Denatured Type I Collagens and the Phenotypic Transition of Rabbit Arterial Smooth Muscle Cells. *Experimental Cell Research* **219**, 249-256 (1995).
44 Vatankhah, E. *et al.* Artificial neural network for modeling the elastic modulus of electrospun polycaprolactone/gelatin scaffolds. *Acta biomaterialia* **10**, 709 (2014).
45 Duan, H. *et al.* Engineering of epidermis skin grafts using electrospun nanofibrous gelatin/ polycaprolactone membranes. *International journal of nanomedicine* **8**, 2077 (2013).
46 Jain, A. *et al.* Guiding intracortical brain tumour cells to an extracortical cytotoxic hydrogel using aligned polymeric nanofibres. *Nature materials* **13**, 308 (2014).
47 Liu, X., Won, Y. & Ma, P. X. Surface modification of interconnected porous scaffolds. *Journal of Biomedical Materials Research Part A* **74A**, 84-91 (2005).
48 Zhang, Q. *et al.* In situ controlled release of rhBMP-2 in gelatin-coated 3D porous poly(ε-caprolactone) scaffolds for homogeneous bone tissue formation. *Biomacromolecules* **15**, 84 (2014).
49 Butler, M. F., Ng, Y.-F. & Pudney, P. D. A. Mechanism and kinetics of the crosslinking reaction between biopolymers containing primary amine groups and genipin. *Journal of Polymer Science Part A: Polymer Chemistry* **41**, 3941-3953 (2003).
50 Nam, J., Huang, Y., Agarwal, S. & Lannutti, J. Improved cellular infiltration in electrospun fiber via engineered porosity. *Tissue engineering* **13**, 2249-2257 (2007).

51 Stephen, J. E. & William, W. S. Statistical geometry of pores and statistics of porous nanofibrous assemblies. *Journal of The Royal Society Interface* **2**, 309-318 (2005).
52 Soliman, S. *et al.* Controlling the porosity of fibrous scaffolds by modulating the fiber diameter and packing density. *Journal of biomedical materials research. Part A* **96**, 566-574 (2011).
53 Stankus, J. J. *et al.* Fabrication of cell microintegrated blood vessel constructs through electrohydrodynamic atomization. *Biomaterials* **28**, 2738-2746 (2007).
54 Laterreur, V. *et al.* Comparison of the direct burst pressure and the ring tensile test methods for mechanical characterization of tissue-engineered vascular substitutes. *Journal of the mechanical behavior of biomedical materials* **34**, 253-263 (2014).
55 Gauvin, R. *et al.* Mechanical Properties of Tissue-Engineered Vascular Constructs Produced Using Arterial or Venous Cells. *Tissue engineering. Part A* **17**, 249-2059 (2011).
56 Chen, Z., Cao, L., Wang, L., Zhu, H. & Jiang, H. Effect of fiber structure on the properties of the electrospun hybrid membranes composed of poly(ε-caprolactone) and gelatin. *Journal of Applied Polymer Science* **127**, 4225-4232 (2013).
57 Yang, F., Xu, C., Kotaki, M., Wang, S. & Ramakrishna, S. Characterization of neural stem cells on electrospun poly(L-lactic acid) nanofibrous scaffold. *Journal of Biomaterials Science, Polymer Edition* **15**, 1483-1483 (2004).
58 International Organization for Standardization, ISO 7198:1998 Cardiovascular implants -- Tubular vascular prostheses. (1998).
59 Donovan, D. L., Schmidt, S. P., Townshend, S. P., Njus, G. O. & Sharp, W. V. Material and structural characterization of human saphenous vein. *Journal of Vascular Surgery* **12**, 531-537 (1990).
60 Karimi, A., Navidbakhsh, M., Shojaei, A. & Faghihi, S. Measurement of the uniaxial mechanical properties of healthy and atherosclerotic human coronary arteries. *Materials science & engineering. C, Materials for biological applications* **33**, 2550 (2013).
61 Feng, B., Tu, H., Yuan, H., Peng, H. & Zhang, Y. Acetic-acid-mediated miscibility toward electrospinning homogeneous composite nanofibers of GT/PCL. *Biomacromolecules* **13**, 3917 (2012).
62 Hotaling, N. A., Bharti, K., Kriel, H. & Simon, C. G. Validated Open Source Nanofiber Diameter Measurement Tool. *Biomaterials* (Submitted, 2015).

63 Pham, Q. P., Sharma, U. & Mikos, A. G. Electrospun poly (ε-caprolactone) microfiber and multilayer nanofiber/microfiber scaffolds: Characterization of scaffolds and measurement of cellular infiltration. *Biomacromolecules* **7**, 2796-2805, (2006).
64 Bulysheva, A. A., Bowlin, G. L., Klingelhutz, A. J. & Yeudall, W. A. Low-temperature Electrospun Silk Scaffold for In Vitro Mucosal Modeling. *Journal of Biomedical Materials Research. Part a* **100**, 757-767, (2012).
65 Ki, C. S. *et al.* Electrospun three-dimensional silk fibroin nanofibrous scaffold. *Journal of Applied Polymer Science* **106**, 3922-3928, (2007).
66 Zander, N. E., Orlicki, J. A., Rawlett, A. M. & Beebe Jr, T. P. Electrospun polycaprolactone scaffolds with tailored porosity using two approaches for enhanced cellular infiltration. *Journal of Materials Science: Materials in Medicine* **24**, 179-187 (2013).
67 Zhang, Y., Ouyang, H., Lim, C. T., Ramakrishna, S. & Huang, Z. M. Electrospinning of gelatin fibers and gelatin/PCL composite fibrous scaffolds. *Journal of Biomedical Materials Research Part B: Applied Biomaterials* **72B**, 156-165 (2005).
68 Ghasemi-Mobarakeh, L., Prabhakaran, M. P., Morshed, M., Nasr-Esfahani, M.-H. & Ramakrishna, S. Electrospun poly(ε-caprolactone)/gelatin nanofibrous scaffolds for nerve tissue engineering. *Biomaterials* **29**, 4532-4539 (2008).
69 Lemire, J. M., Covin, C. W., White, S., Giachelli, C. M. & Schwartz, S. M. Characterization of cloned aortic smooth muscle cells from young rats. *American Journal of Pathology* **144**, 1068-1081 (1994).
70 Blackstone, B. N. *et al.* Plasma surface modification of electrospun fibers for adhesion-based cancer cell sorting. *Integrative Biology* **4**, 1112-1121, (2012).
71 Sheets, K., Wunsch, S., Ng, C. & Nain, A. S. Shape-dependent cell migration and focal adhesion organization on suspended and aligned nanofiber scaffolds. *Acta biomaterialia* **9**, 7169 (2013).
72 Berry, C. Design and Development of Two Test Fixtures to Test the Longitudinal and Transverse Tensile Properties of Small Diameter Tubular Polymers. *Dissertation/Thesis thesis, DigitalCommons@CalPoly* (2011)
73 Xu, C. Y., Inai, R., Kotaki, M. & Ramakrishna, S. Aligned biodegradable nanofibrous structure: a potential scaffold for blood vessel engineering. *Biomaterials* **25**, 877-886, (2004).

74 Schnell, E. *et al.* Guidance of glial cell migration and axonal growth on electrospun nanofibers of poly-ε-caprolactone and a collagen/poly-ε-caprolactone blend. *Biomaterials* **28**, 3012-3025, (2007).
75 Jia, L., Prabhakaran, M. P., Qin, X. & Ramakrishna, S. Guiding the orientation of smooth muscle cells on random and aligned polyurethane/collagen nanofibers. *Journal of Biomaterials Applications* **29**, 364-377 (2014).
76 Pan, S. *et al.* Evaluation of an immune-privileged scaffold for In vivo implantation of tissue-engineered trachea. *Biotechnol Bioproc E* **19**, (2014).
77 Wang, Y. *et al.* Electrospun tubular scaffold with circumferentially aligned nanofibers for regulating smooth muscle cell growth. *ACS applied materials & interfaces* (2014).
78 Jana, S., Cooper, A., Ohuchi, F. & Zhang, M. Uniaxially aligned nanofibrous cylinders by electrospinning. *ACS applied materials & interfaces* (2012).
79 Wu, H., Fan, J., Chu, C.-C. & Wu, J. Electrospinning of small diameter 3-D nanofibrous tubular scaffolds with controllable nanofiber orientations for vascular grafts. *Journal of Materials Science: Materials in Medicine* **21**, 3207-3215, (2010).
80 Baji, A., Mai, Y.-W., Wong, S.-C., Abtahi, M. & Chen, P. Electrospinning of polymer nanofibers: Effects on oriented morphology, structures and tensile properties. *Composites Science and Technology* **70**, 703-718, (2010).
81 Kang, I.-K., Kwon, B. K., Lee, H. B. & Lee, J. H. Immobilization of proteins on poly(methyl methacrylate) films. *Biomaterials* **14**, 787-792, (1993).
82 Gümüşderelioğlu, M. & Türkoğlu, H. Biomodification of non-woven polyester fabrics by insulin and RGD for use in serum-free cultivation of tissue cells. *Biomaterials* **23**, 3927-3935, (2002).
83 Lü, X., Li, D., Huang, Y. & Zhang, Y. Application of a modified Coomassie brilliant blue protein assay in the study of protein adsorption on carbon thin films. *Surface & Coatings Technology* **201**, 6843-6846, (2007).
84 Chen, T.-C., Lai, C.-H., Chang, J.-L. & Chang, S.-W. Mitomycin C Retardation of Corneal Fibroblast Migration via Sustained Dephosphorylation of Paxillin at Tyrosine 118. *Investigative Ophthalmology & Visual Science* **53**, 1539-1547 (2012).
85 Dikina, A. D., Strobel, H. A., Lai, B. P., Rolle, M. W. & Alsberg, E. Engineered cartilaginous tubes for tracheal tissue replacement via self-assembly and fusion of human mesenchymal stem cell constructs. *Biomaterials* **52**, 452-462 (2015).

Appendix A: Attachment assay standard curves

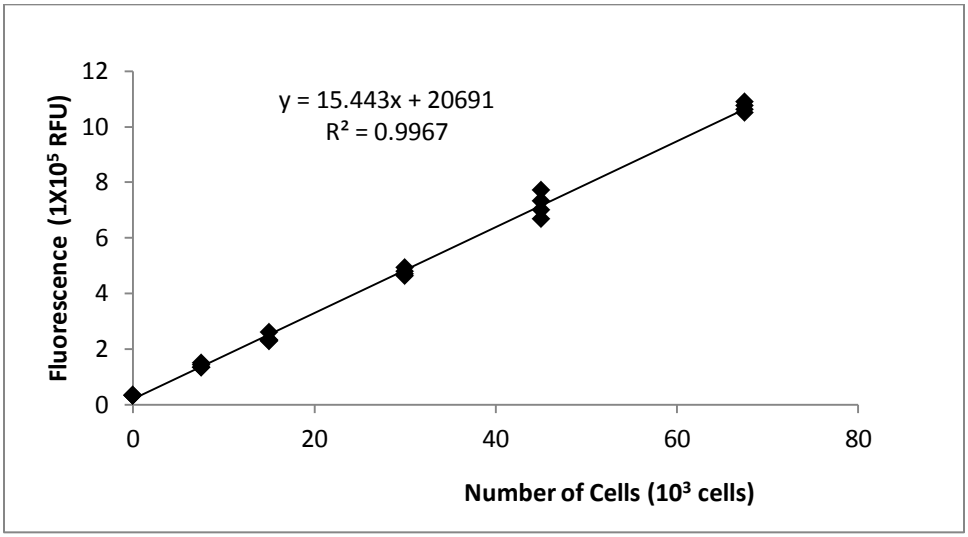

AlamarBlue® fluorescence standard curve (for first experimental trial) Standard curve relating cell number and relative fluorescence units (RFU) using AlamarBlue® assay. 2 samples of known cell numbers and two replicates were analyzed per sample. Standard linear regression model is displayed in black on the plot, with coefficient of determination (R^2) and equation for the model.

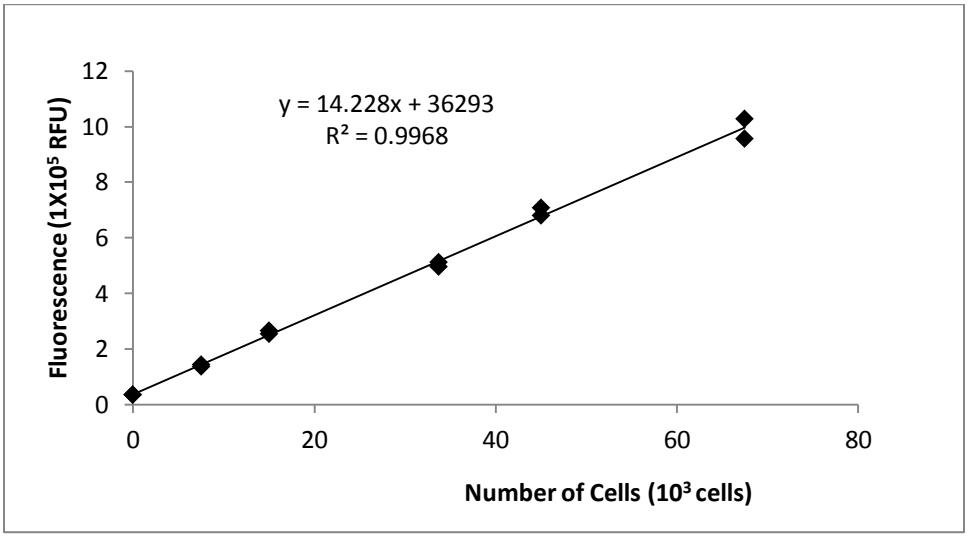

AlamarBlue® fluorescence standard curve (for first experimental trial) Standard curve relating cell number and relative fluorescence units (RFU) using AlamarBlue® assay. 2 Samples of known cell numbers and two replicates were analyzed per sample. Standard linear regression model is displayed in black on the plot, with coefficient of determination (R^2) and equation for the model.

Appendix B: CAD drawings of custom mechanical testing grips

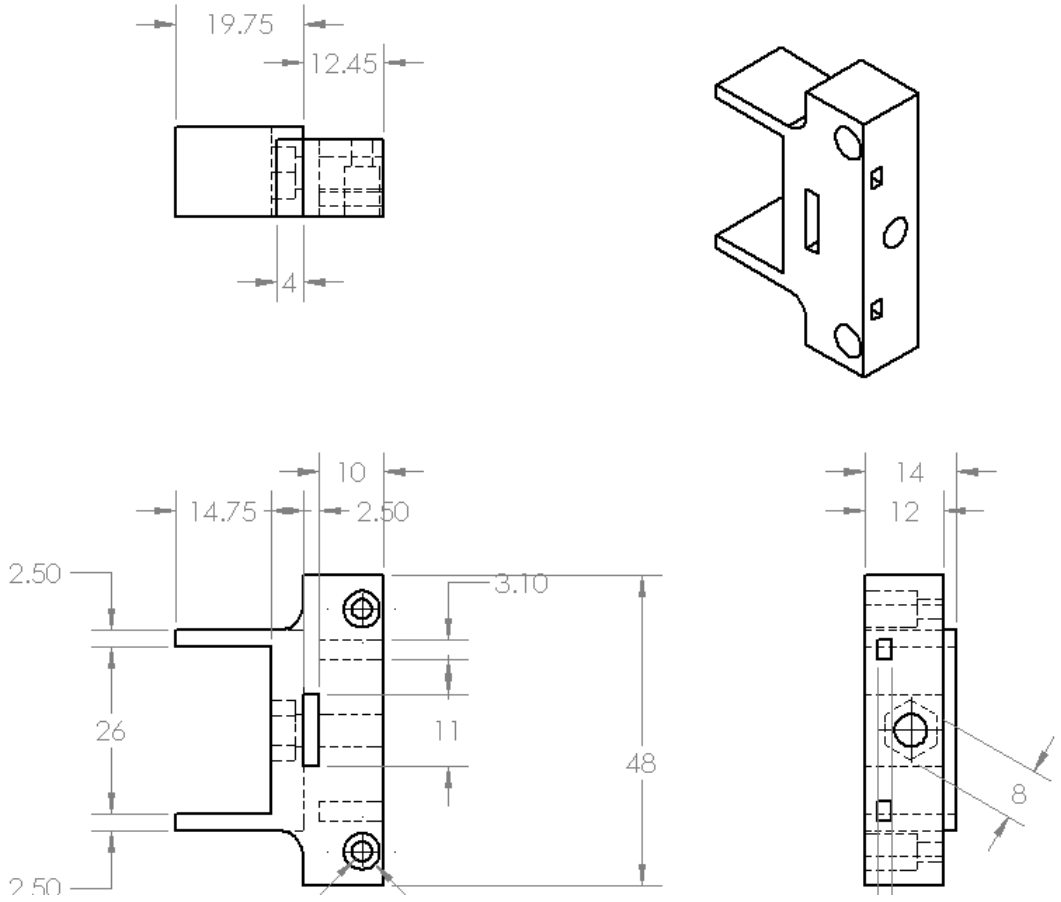

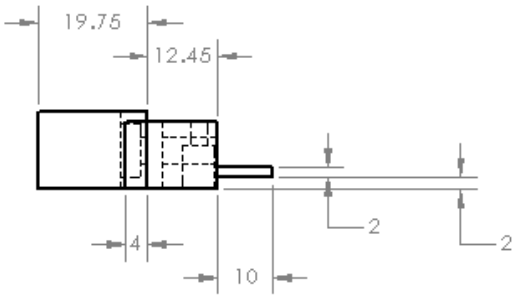
19.75
12.45
2
2
4
10

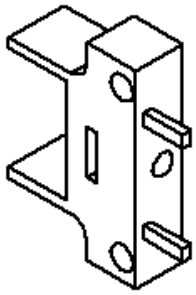

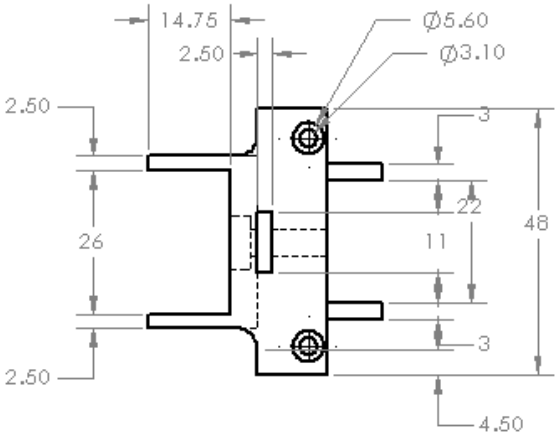
14.75
2.50
Ø5.60
Ø3.10
2.50
3
22
48
26
11
3
2.50
4.50

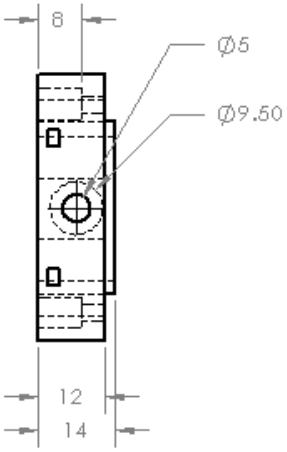
8
Ø5
Ø9.50
12
14

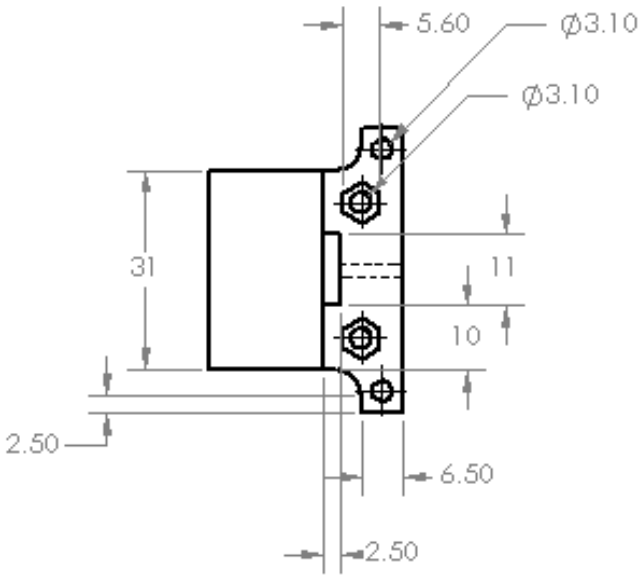
5.60
Ø3.10
Ø3.10
31
11
10
2.50
6.50
2.50

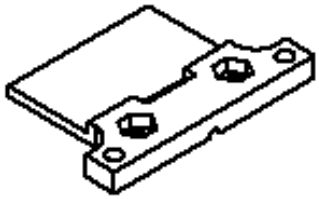

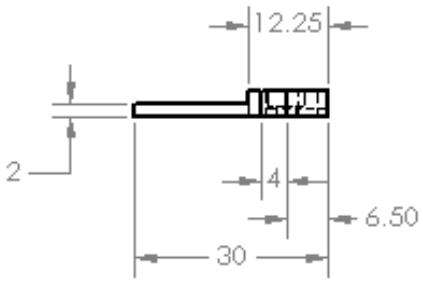
12.25
2
4
6.50
30

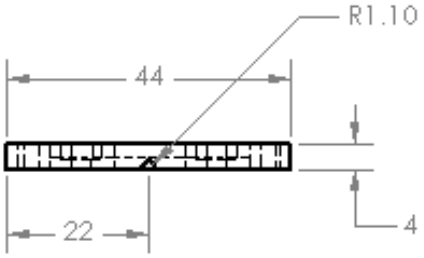
R1.10
44
22
4

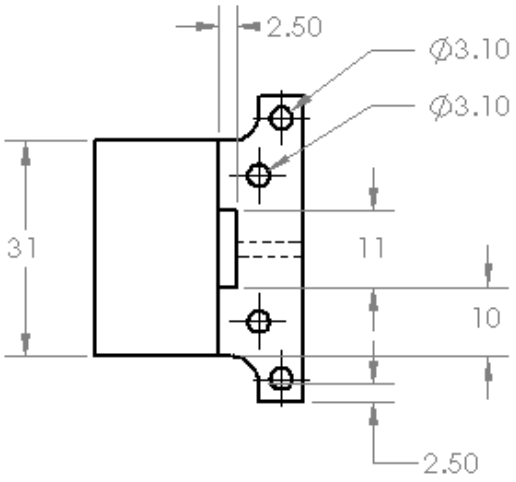
2.50
Ø3.10
Ø3.10
31
11
10
2.50

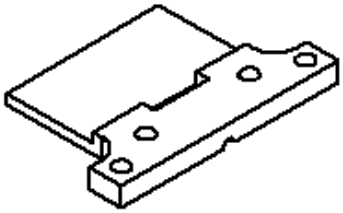

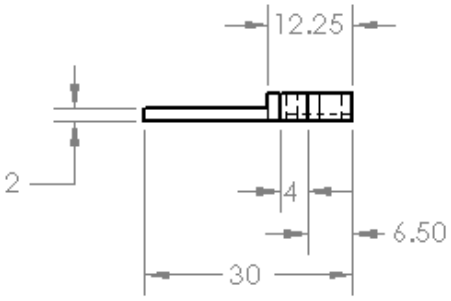
12.25
2
4
6.50
30

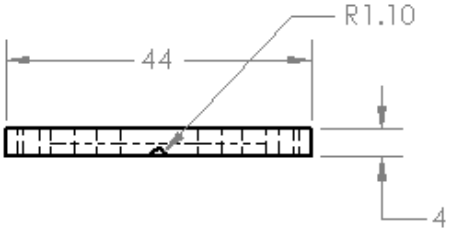
R1.10
44
4

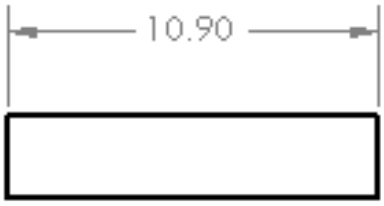
10.90

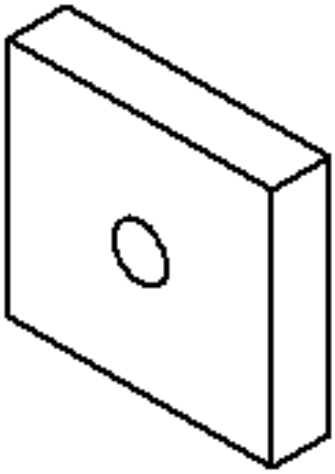

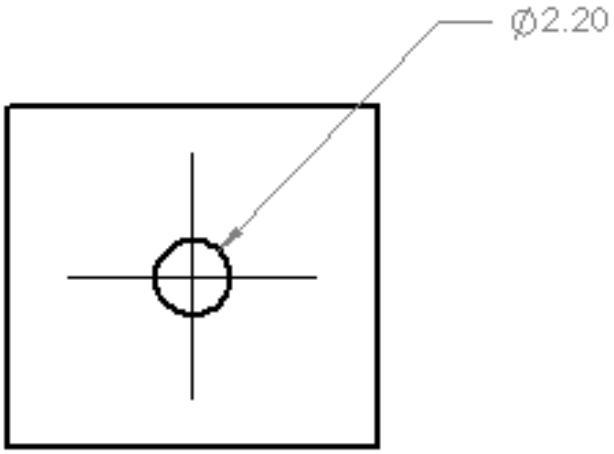
Ø2.20

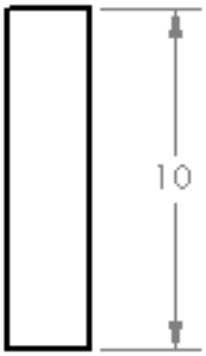
10